A Thesis for the Doctor of Philosophy

OT-55 and epigenetic regulator martinostat induce immunogenic cell death in imatinib-sensitive and –resistant chronic myeloid leukemia

OT-55 와 후성 유전 조절 물질 martinostat 의 면역 세포 사멸을 통한 imatinib 민감성 및 저항성 만성 골수성 백혈병 (chronic myeloid leukemia)의 표적 항암 치료

August, 2018

Aloran Mazumder

College of Pharmacy

Seoul National University

OT-55 and the epigenetic regulator martinostat induce immunogenic cell death in imatinib-sensitive and -resistant chronic myeloid leukemia

OT-55와 후성 유전 조절 물질 martinostat의 면역 세포 사멸을 통한 imatinib 민감성 및 저항성 만성 골수성 백혈병 (chronic myeloid leukemia)의 표적 항암 치료

지도교수 Marc Francois Diederich

이 논문을 약학박사 학위논문으로 제출함

2018 년 8 월

서울대학교 대학원
약학과 의약생명과학 전공
Aloran Mazumder

Aloran Mazumder의 약학박사 학위논문을 인준함

2018 년 8 월

위 원 장	이 정 원	(인)
부위원장	서 영 준	(인)
위 원	한 병 우	(인)
위 원	나 혜 경	(인)
위 원	Marc Francois Diederich	(인)

OT-55 and the epigenetic regulator martinostat induce immunogenic cell death in imatinib-sensitive and -resistant chronic myeloid leukemia

by

Aloran Mazumder

A dissertation submitted to the College of Pharmacy in partial fulfillment of the requirements for the degree of

DOCTOR OF PHYLOSOPHY

(Major: Pharmaceutical Bioscience)

Seoul National University

Seoul, South Korea

August, 2018

APPROVED:

Advisory Committee Chair, Jung Weon Lee

Advisory Committee Vice-Chair, Young-Joon Surh

Byung Woo HAN

Advisory Committee, Byung Woo Han

Advisory Committee, Hye-Kyung Na

Advisory Committee, Marc Francois Diederich

OT-55 and epigenetic regulator martinostat induce immunogenic cell death in imatinib-sensitive and –resistant chronic myeloid leukemia

by

Aloran Mazumder

A thesis submitted in partial fulfillment of the

requirements

for the degree of

DOCTOR OF PHILOSOPHY

(Pharmacy: Pharmaceutical bioscience major)

Under the supervision of

Professor Marc Francois Diederich

College of Pharmacy

Seoul National University

August, 2018

ABSTRACT

Immunogenic cell death (ICD) has emerged as a sequence of events that engages the adaptive arm of the immune system. Depending upon the initial stimulus, cancer cell death can be defined as ICD, which is characterized by a sequence of events involving changes on the cell surface and a release of damage-associated molecular patterns. This phenomenon engages the macrophages and dendritic cells of the immune system to act against cancer.

In the present study, we found that a bis(4-hydroxycoumarin) derivative, OT-55, and the histone deacetylase inhibitor martinostat triggered ICD in chronic myeloid leukemia (CML) cells in an endoplasmic reticulum ER stress-dependent manner. We provide the first demonstration of ICD induction in cells harboring the T315I mutation. OT-55 inhibited tumor necrosis factor α-induced activation of nuclear factor-κB and produced synergistic effects when used in combination with imatinib to inhibit tumor formation by CML primary blasts in an in vivo zebrafish model. Furthermore, OT-55 synergized with omacetaxine in T315I-mutant cells to inhibit the expression of myeloid cell leukemia 1, thus triggering apoptosis. OT-55 targeted CML cells with stem-like characteristics by attenuating their elevated aldehyde dehydrogenase activity and mitochondrial oxidative metabolism.

Compared to vorinostat, martinostat increased acetylation levels, reduced cell proliferation, viability, and colony formation of CML cells at a much lower concentration. It showed synergistic cytotoxicity in combination with imatinib in both imatinib -sensitive and –resistant CML cells.

TABLE OF CONTENTS

LIST OF ABBREVIATIONS

AIF: Apoptosis inducing factor

ATP: Adenosine triphosphate

BAX: BCL2 Associated X protein

Bcl-2: B-cell lymphoma 2

Bcl-xL: B-cell lymphoma extra large

CD: Cluster of differentiation

CML: Chronic myeloid leukemia

CRT: Calreticulin

DAMPS: Damage-associated molecular patterns

DC: Dendritic cell

DNA: Deoxyribonucleic acid

ER: Endoplasmic reticulum

ERp57: Endoplasmic-reticulum-dependent protein disulfide isomerase

GRP57: Endoplasmic-reticulum Protein 57

HDAC: Histone deacetylase

HMGB1: High-mobility group box 1

ICD: Immunogenic cell death

IL: Interleukin

IFN: Interferon

JNK: c-Jun N-terminal kinase

Mcl-1: Myeloid leukemia cell differentiation protein

NF-κB: Nuclear factor kappa B

NK cells: Natural killer cells

NKT cells: Natural killer T cells

PRIMA 1: P53 reactivation and induction of massive apoptosis

RIP: Receptor-interacting protein

RNA: Ribonucleic acid

STAT: Signal transducer and activator of transcription

TA: Tumor antigen

TNF: Tumor necrosis factor

TRADD: Tumor necrosis factor receptor type 1-associated DEATH domain protein

TRAF2: TNF receptor-associated factor 2

TRAIL: TNF-related apoptosis-inducing ligand

LIST OF FIGURES

INTRODUCTION

1. Cancer-associated cell death

Cell death or programmed cell death is a cascade of biological events that eliminate damaged cells and play an important role during normal cell turnover, development, functioning of the immune system, hormone-dependent atrophy, and preservation of tissue homeostasis. On the basis of the hallmarks of cancer proposed by Douglas Hanahan and Robert Weinberg, Douglas Green and Gerard Evan explained that the core changes that convert a normal cell into a malignant one might simply be increased proliferation coupled with decreased cell death [1]. Therefore, dysfunction in programmed cell death is the major cause of cancer and accumulating evidence suggests that cell death is closely related to anti-cancer therapy. Several nomenclatures have been proposed to classify the different types of programmed cell death however, the most widely accepted ones are apoptosis, autophagy, and necrosis [1].

The basic understanding of apoptosis in the mammalian cell emerged from the investigation of cell death that occurs during the development of nematodes [2]. Since then, apoptosis has been studied extensively to understand the underlying mechanism and its pivotal in the pathogenesis of different diseases including cancer. Apoptosis is characterized by ordered and orchestrated

biochemical events including the activation of proteases that lead to inter-nucleosomal DNA fragmentation [2]. Apoptosis can be initiated by two pathways involving either activation of death receptors [such as the TNF (tumor necrosis factor) family of cytokine receptors] or a release of pro-apoptotic proteins such as cytochrome c from the mitochondria. The key players in both the pathways are caspases (the cysteine-dependent, aspartate-specific family of proteases) [3]. Moreover, the mitochondrial dynamics contribute substantially to the initiation of apoptosis [1].

Cancer cells accumulate gene mutations by different molecular mechanisms that contribute to failure of the apoptotic pathways and lead to carcinogenesis. Cancer cells can overexpress antiapoptotic proteins such as Bcl-2 or downregulate proapoptotic Bax. The expression of both is regulated by a tumor suppressor gene p53 which undergo mutation in 50% of all types of human tumors. PRIMA 1 (P53 reactivation and induction of massive apoptosis) is a compound that is currently being tested in a clinical trial and restores the tumor suppressor function of mutant p53 by covalently modifying the core domain of mutated p53 through alkylation of thiol groups [4]. It is also one of the unique chemotherapeutic agents because it does not affect on wild-type p53. Another approach to the induction of apoptosis in cancer cells is to target proteins of the Bcl-2 family proteins by means of BH3 mimetics, which bind to the pocket of Bcl-2 where normally BH3 proteins would bind. Navitoclax

(ABT-263) and venetoclax (ABT-199) have shown efficacy in preclinical and clinical trials [5]. Moreover, in hematological cancers including acute myeloid leukemia, where overexpression of Bcl-2 is a major cause of poor prognosis, synergistic anticancer effect of a combination with Mcl-1 inhibitor have been reported [6].

Autophagy is a cellular metabolic process where proteins and organelles are engulfed by autophagosomes, digested in lysosomes, and recycled to maintain cellular homeostasis [1]. In cancer, autophagy plays a dual role. Its activation in response to cellular stress can enable cell survival by maintaining the energy production that can lead to therapeutic resistance. In contrast, rapid onset of autophagy under the influence of external stimuli may remove damaged organelles and proteins, thereby limiting genomic instability and eventually leading to cell death [1]. In apoptosis-defective cells, autophagy inducing agents are used to accumulate excessive cellular damage, and progressive autophagy naturally designed to alleviate that damage can lead to autophagic cell death. Nonetheless, autophagy inhibitors such as chloroquine and hydroxychloroquine are currently being tested clinical trials against various cancers to overcome the autophagy-induced therapeutic resistance [7].

The lack of caspase activity and lysosomal involvement distinguishes necrosis from apoptosis and autophagy. Necrosis is mainly characterized by early swelling of intracellular organelles such as mitochondria, the endoplasmic

reticulum and, Golgi apparatus followed by a loss of cell membrane integrity eventually leading to cell death [8]. Various proteins such as TRAIL, TRADD, TRAF2, JNK1, RIP1, XRCC1, AIF, calpains, Bax, or Drp1 have been implicated in necrotic cell death [8]. Moreover, necrotic cells can trigger an inflammatory response via a release of nuclear factors such as high mobility group box 1 (HMGB1) [9]. Shikonin, a natural naphthoquinone pigment purified from *Lithospermum erythrorhizon*, induces necrosis in various cancer types [10].

2. Immune surveillance against cancer

Cancer immune surveillance is defined as a host protective process designed to inhibit carcinogenesis. The interaction of host and tumor cells includes three essential phases: elimination, equilibrium, and escape which are often referred to as the *three Es* [11]. The process of elimination includes both an innate and adaptive response. Effector cells of the immune system such as natural killer (NK), natural killer T cells (NKT) and γδT cells are activated by the cytokines released from tumor cells. This event in turn recruit additional immune cells, which release proinflammatory cytokines including IL-2 and interferon γ. NK cells in the process of killing tumor cells release tumor antigens (TAs) which activate the adaptive immune response [11].

In the process of equilibrium, a tumor produces cells resistant to immune effector cells. These cells have the ability to develop more efficiently in an immunocompetent individual. Random gene mutations within tumor cells allow for the development of tumor cell variants that are less immunogenic, and the process may proceed for many years. During this process, lymphocytes and interferon γ exert immune selection pressure on tumor cells.

The process of escape is defined as alterations in signal transduction molecules of the effector cells. The lack of TA recognition by the effector cells due to alterations impair the immune response against cancer. Loss of the CD3-ζ chain of tumor infiltrating lymphocytes (TILs) has been attributed to immune evasion in cooperation with immunosuppressive cytokines and impairment of TILs. It has also been reported that the loss of CD3-ζ correlates with increased levels of TGF-β and downregulation of interferon γ [11].

3. Immunogenic cell death

Homeostatic cell death, which mainly takes place via apoptosis, can be tolerogenic (promoting tolerance to self) or neutral (exerting no effect on the immune system) [12]. Nonetheless, the past few years have witnessed a new concept, ICD, which is defined as a cell death modality that stimulates an immune response against the dying cancer cells [13]. The concept of ICD was proposed based on the clinical evidence where chemotherapy administration

induced a tumor- specific anticancer response which supplements the conventional effect of cytotoxic drugs. Some anti-cancer agents reorchestrate the composition of immune infiltrate of the tumor, and this change improves the outcome of the therapy [14]. After ICD, the immune response is initiated by the dendritic cells (DCs) which engulf and present the antigen from a dying tumor cell. Different biochemical assays have revealed a few hallmarks of ICD. Preapoptotic display of calreticulin (CRT), or other endoplasmic-reticulum proteins such as ERp57 on the cell surface as well as the secretion of ATP and a nonhistone chromatin protein called high mobility group box 1 (HMGB1) are the major characteristic features of ongoing ICD [15].

ICD is a consequence of two types of cellular stress: ER stress and autophagy [12]. As a consequence of ER stress, CRT, which is mainly located in the ER lumen, is translocated to the cell surface: a phenomenon that occurs before the cells are committed to apoptosis. Ectopic expression of CRT acts as an "eat me signal" for DCs to engulf the tumor cells. Studies have shown that blockade of CRT exposure reduces the efficacy of ICD-inducing drugs such as anthracyclines in immunocompetent mice [16]. Cells with CRT exposed on the surface are engulfed by CD91- positive cells such as macrophages and DCs. It is then processed to present the antigen and to initiate a cognate immune response [17]. CRT exposure has been linked to patients' survival in different ways. In non-Hodgkin lymphoma, a combination of heat shock, γ-

radiation, and ultraviolet C light induces CRT exposure, which allows DCs to initiate an immune response [17]. In acute myeloid leukemia, the display of CRT by leukemic cells predicts a T-cell response that improves patients' survival [18].

Inhibition of autophagy neither affects the exposure of CRT nor the release of HMGB1; however, it prevents the release of ATP from the dying cancer cells because autophagy-competent, but not autophagy deficient, tumors recruit DCs [12]. In autophagy deficient cancers, this problem can be overcome by inhibiting extracellular ATP-degrading enzymes, and this action results in increased pericellular ATP concentration. Often cells that are under physical or chemical stress because of hypoxia or exposure to cytotoxic drugs undergo mechanical distortion and damage in the plasma membrane, and consequently ATP is released. The latter process happens via different mechanisms including exocytosis of ATP within ATP-containing vesicles, or secretion of cytoplasmic ATP by gap junctions and transporters of the ATP binding cassette family (ABC) family. In cancer cells, ATP is released after caspase 3 or 7 activation and cleavage of pannexin 1. Extracellular ATP acts as a chemoattractant for monocytes that initiate an immune response [12]. It binds to receptors P2Y2 which is expressed on cells of the myeloid lineage. The inhibition of P2Y2 by suramin treatment impairs the engulfment of dying thymocytes by macrophages [19]. Additionally, ATP affects the function of

immune effectors. An ATP release in vitro has been shown to promote formation of lamellipodial membrane protrusions, which cause the spreading of macrophages [20]. In vivo intradermal injection of ATPγS (an analog of ATP) increases the expression of class 11 MHC molecules, CD80, CD86, IL-1β and IL-12 [21].

HMGB1 is the most abundant nonhistone chromatin protein, which is expressed by all nucleated cells. In response to many antineoplastic agent, HMGB1 is released as a result of a loss of plasma membrane integrity. It activates proinflammatory responses by signaling through receptors that are expressed on both immune and nonimmune cells [12]. It binds to TLR-4 activating the release of proinflammatory cytokines by monocytes or macrophages.

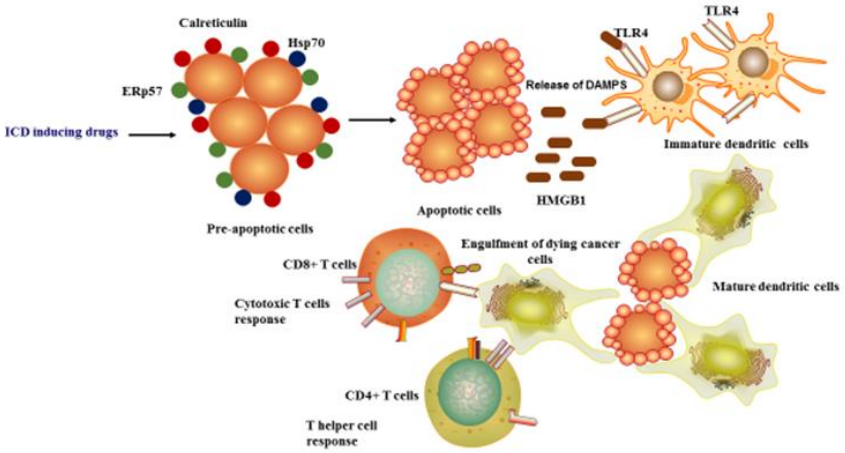

Figure 1. 1: Immunogenic cell death response (ICD).

This scheme presents ICD response to ICD- inducing drugs. Ectopic expression of calreticulin, ERp57, and Hsp70 by pre-apoptotic cells comes first. A release of HMGB1 happens next, which binds to receptor TLR4 present on DCs and triggers an ICD response. The dying cancer cells are engulfed by the DCs and are presented to CD8+ T cells and CD4+ T cells to initiate an immune response.

HMGB1 can associate with CXCL12 thereby, signaling through CXCR4 and promoting the recruitment of mononuclear cells to the tumor site. TLR-4 and its adaptor Myd88 are essential for initiation of ICD against cancer cells because tumors that develop in mice with TLR-4 knockout or Myd88 knockout are less responsive to ICD-inducing agents such as anthracyclines as compared to tumors growing in wild-type immunocompetent mice [12].

Moreover, HMGB1-when binding to TLR-4 expressing DCs it increases the expression of pro-IL-1β. The latter, after maturs to IL-1β prevents the lysosomal degradation of engulfed TAs which is required for cross presentation to activate an immune response. Therefore, the binding of HMGB1 to TLR4 is a prerequisite of active ICD.

4. Chronic myeloid leukemia (CML)

CML or chronic granulocytic leukemia is a slowly progressing blood and bone marrow disorder where the bone marrow produces too many white blood cells. The disease is caused by a fusion onco-protein Bcr-Abl in Philadelphia chromosome. Short pieces of chromosome 9 and 22 break off and the piece of chromosome 9 attaches to chromosome 22. This newly formed chromosome is called Philadelphia chromosome [22]. CML is one of the first cancers associated with a specific chromosomal aberration. Traditionally, the disease was treated with conventional chemotherapy involving hydroxyurea or busulfan. These agents can increase patients' survival however the chromosomal aberration is still evident. Interferon-α provides a survival advantage in patients and allogeneic bone marrow transplant was reported to be curative in some patients [22]. Imatinib mesylate a synthetic tyrosine kinase inhibitor, was developed to target the Bcr-Abl fusion protein. It dramatically increased patients' survival and is well tolerated by patients. It remains a first

line treatment for patients with CML. In 85% to 90% of patients, the disease is detected in the chronic phase where imatinib is very effective, but the disease progresses to the accelerated phase and the blast crisis phase within 5 years. The progression of the disease from one phase to another is complex and varies among individual patients. Patients with mutation in one of the kinase domains (Y253F/H, E255K/V, T315I, H396P/R43,44, M244V, M351T or F359V) do not respond to imatinib treatment [22]. Nilotinib and dasatinib, next generation tyrosine kinase inhibitors, which are structurally similar to imatinib but have greater affinity for Bcr-Abl and inhibit Src family kinases, were designed to overcome imatinib resistance in CML. These agents have improved the survival but a complete molecular response is not achieved [23].

5. Immune surveillance in CML

The activity of a patient's own immune system in recognizing the the Bcr-Abl-positive cells and whether the activity can be boosted is currently investigated in vaccination studies; however, the results have not been very convincing [24]. In both hematological and solid tumors, the action of CD8+ cytotoxic T lymphocytes is considered most important for induction of antitumor immune response, along with CD4+ T helper cells, which are involved in the induction and maintenance of cytotoxic T-lymphocyte responses, interaction with effector cells, and production of cytokines such as IL-2 and interferon γ. To

evade the immune response, cancer cells, resort to major histocompatibility complex (MHC) class II (MHC II) downregulation, thereby reducing the host immune response to the tumor. An increased clinical benefit has been observed in patients whose tumors show higher MHC II expression [24]. In CML, stem progenitor cells, which are characterized by the expression of CD34 and Bcr-Abl and are resistant to tyrosine kinase inhibitors show a downregulation of MHC II as a mechanism of evasion of the immune response [24].

CHAPTER I

The bis(4-hydroxycoumarin), OT-55, induces immunogenic cell death in imatinib-sensitive and -resistant chronic myeloid leukemia

1. Purpose of this study

Chronic myeloid leukemia (CML) is defined as a myeloproliferative disorder that originates in hematopoietic stem cells as a result of the expression of oncogenic Bcr-Abl. Imatinib and other tyrosine kinase inhibitors (TKIs) such as nilotinib and dasatinib have dramatically improved patient survival. However, disease progression towards an accelerated blastic phase, with the acquisition of additional TKI-resistant mutations, is observed in 20 30% of CML patients, and is associated with therapeutic failure [25].

The most clinically relevant mutation, T315I, is reported in 15 20% of patients with relapsed disease. In 2012, ponatinib was approved by the U.S Food and Drug Administration for the treatment of patients with T315I mutation. However, this was suspended in 2013 because of toxicity [26]. The use of omacetaxine in patients with T315I mutation attracted interest because its mechanism of action was independent of the ATP binding domain and Bcr-Abl mutations [25]. However, the efficacy of this treatment can be limited by a small population of primitive CD34+/Bcr-Abl+ cells with stem cell characteristics; these can remain quiescent and non-responsive to TKIs [27]. Together, these reports suggest that an effective treatment for CML can only be achieved by molecules that can target critical mutations and rare stem cell

sub-populations, whether administered individually or in combination with other novel compounds.

Transcription factors such as nuclear factor-κB (NF-κB) and signal transducer and activator of transcription (STAT) have been shown to be essential regulators of CML development and progression. However, the problems associated with targeting transcription factors directly have led to the investigation of epigenetic regulators such as JQ1, a thienotriazolodiazepine inhibitor of the bromodomain and extra terminal (BET) family proteins that can inhibit the NF-κB and STAT pathways in a range of different malignancies [28]. In addition, immunogenic cell death (ICD) has emerged as an essential component of therapy-induced anti-tumor immunity in both solid and hematological malignancies. Cancer cell death in response to a selective agent can be defined as either immunogenic or non-immunogenic, depending on the changes in the composition of the cell surface and release of soluble mediators that act on dendritic cell receptors [12]. Natural and synthetic molecules that produce anti-cancer effects on TKI-resistant CML by various mechanisms have been identified. Omacetaxine is one such naturally occurring compound, discovered in Cephalotaxus harringtonia. Inspired by the biscoumarin structure of the naturally occurring anti-tumor compound, dicoumarol and consistent with our long-standing interest in synthetic coumarins with anti-cancer potential [29]. The present study describes the novel bis(4-

hydroxycoumarin) compound, OT-55, 3,3'-[3-(5-chloro-2-hydroxyphenyl)-3-oxopropane-1,1-diyl]bis(4-hydroxycoumarin). This compound, which has potent anti-cancer activity mediated via the induction if ICD in CML, synergizes with imatinib and omacetaxine in imatinib-sensitive and -resistant cell lines, as well as in primary patient blasts.

2. Materials and methods

2.1. Chemistry

3,3'-[3-(5-chloro-2-hydroxyphenyl)-3-oxopropane-1,1-diyl]bis(4-hydroxycoumarin) OT-55 has been synthetized according to our previously reported procedure. The reaction of 4-hydroxycoumarin 1 with ω-formyl-5'-chloro-2'-hydroxyacetophenone 2 catalyzed by 4-pyrolidinopyridine (4-PPy) in refluxing chloroform, has led to the desired OT-55 in 68% yield. The product was purely isolated after solvent removal under vacuum and direct recrystallisation from ethanol.

2.2. Cell culture and treatment

Chronic myeloid leukemia cell lines K562 and MEG-01 were purchased from Deutsche Sammlung für Mikroorganismen und Zellkulturen (DSZM; Braunschweig, Germany) and cultured in RPMI medium (Lonza, Basel, Switzerland) supplemented with 10% (v/v) fetal calf serum (FBS) (Biowest, Nuaille, France) and 1% (v/v) antibiotic–antimycotic (Lonza, Basel,

Switzerland) at 37 °C and 5% of CO2. KBM-5 cells were kindly donated by Dr. Bharat B. Aggarwal and KBM-5. KBM-5-T315i cells were developed by culturing the cells with imatinib. Imatinib concentration was increased eventually from 0.25, 0.5 and finally cultured with 1 μM of in IMDM media supplemented with 10% (v/v) fetal calf serum and 1% (v/v) antibiotic–antimycotic. K562R cells were a gift of the Catholic University, Seoul and cultured in RPMI medium with 25 mM HEPES (Lonza, Basal, Switzerland) supplemented with 10% (v/v) FBS and 1% (v/v) antibiotic-antimycotic. Both resistant cells were cultured with 1 μM of imatinib and washed three times before experiment.

2.3. Human primary sample

Human leukemia samples were obtained from the Seoul National University Children's Hospital. The Institutional Review Board (IRB) of Seoul National University Hospital (IRB No. H-1609-133-797) reviewed and approved the study protocol, and exempted the study from the obligation to obtain informed consent. This study was performed following World Medical Association's Declaration of Helsinki.

2.4. Cell Proliferation and viability

Cell proliferation and viability were measured by using the trypan blue exclusion assay (Lonza, Basel, Switzerland). The number of cells per mL was

counted, and the fraction of trypan blue-positive cells was estimated by using a Malassez cell counting chamber (Marienfeld, Lauda-Königshofen, Germany).

2.5. Cell cycle distribution

For cell cycle analysis, cells were collected and fixed in 70% ethanol. DNA was stained with a propidium iodide (PI) solution (1 μg/mL, Sigma-Aldrich, St. Luis, Missouri, USA) in 1x PBS (Hyclone), supplemented with RNase A (100 μg/mL; Roche, Basel, Switzerland). Samples were analyzed by flow cytometry using a FACS CaliburTM system, Becton Dickinson (BD) Biosciences (FACS) (San Jose, CA, USA). Data were recorded statistically (20,000 events/sample) using the Cell Quest software (BD Biosciences) and analyzed using Flow-Jo 8.8.5 software (Tree Star, Inc., Ashland, OR, USA).

2.6. Protein extraction and western blot

Whole cell extracts were prepared using M-PER® (Thermofisher, Waltham, Massachusetts, USA) supplemented with 1x protease inhibitor cocktail (Complete EDTA-free, Roche, Basel, Switzerland) according to the manufacturer's instructions. Proteins were resolved by SDS-PAGE and transferred to PVDF membranes (GE Healthcare, Little Chalfont, UK). Membranes were incubated with selected primary antibodies (Supplementary Table I). Chemo-luminescence signal was detected with the ECL Plus Western

Blotting Detection System (GE Healthcare, Little Chalfont, UK) and quantified by ImageQuant LAS 4000 mini system (GE Healthcare).

2.7. Evaluation of apoptosis and necrosis

The percentage of apoptotic cells was quantified as the fraction of cells showing fragmented nuclei, as assessed by fluorescence microscopy (Nikon, Tokyo, Japan) after staining with Hoechst 33342 (Sigma-Aldrich) and propidium iodide (Sigma-Aldrich). Apoptosis was also confirmed by annexin V/propidium iodide staining and fluorescence-activated cell sorter (FACS) analysis according to the manufacturer protocol (BD Biosciences).

2.8. Colony formation assay

For colony formation assays, 103 cells/mL were grown in a semi-solid methylcellulose medium (Methocult H4230, StemCell Technologies Inc., Vancouver, Canada) supplemented with 10% FBS and indicated concentrations. Colonies were detected after 10 days of culture by adding 1 mg/mL of 3-(4,5-dimethylthiazol-2-yl)-2,5-diphenyltetrazolium bromide (MTT) reagent (Sigma) and were scored by Image J 1.8.0 software (U.S. National Institute of Health, Bethesda, MD, USA).

2.9. Transient transfection and luciferase reporter gene assay

Cells were transiently transfected with 5 μg of a luciferase reporter gene construct containing five repeats of a consensus NF-κB binding site (Stratagene) and 5 μg of a Renilla luciferase control reporter plasmid (ph-RG-TK, Promega, Leiden, Netherlands) and reporter gene assays were carried out. Experiment was conducted as previously described.

2.10. Analysis of immunogenic cell death markers calreticulin and ectopic expression of ERp57

10^6 cells were cultured and treated at indicated concentrations of OT-55 for 24 h. Cells were collected, washed twice with 1x PBS and fixed in 0.25% paraformaldehyde in 1x PBS for 5 min. After washing again twice in cold PBS, cells were incubated for 30 minutes with the primary antibody for calreticulin or ERp57, diluted in cold blocking buffer (2% FBS in 1x PBS), followed by washing and incubation with the Alexa488-conjugated monoclonal secondary antibody in a blocking buffer (for 30 min). Each sample was then analyzed by FACS and fluorescence microscopy to identify cell surface CRT or ERp57. Isotype-matched IgG antibodies were used as a control.

2.11. Detection of HMGB1 release

Cells were seeded in 1 mL of medium. After 24 h, cells were centrifuged, the supernatant was collected and immediately stored at -80 ºC. Quantification of

HMGB1 release in the supernatants was assessed by enzyme-linked immunosorbent assay kit from Shino-Test-Corporation (Jinbocho, Chiyoda-ku, Tokyo, Japan) according to the manufacturer's instructions.

2.12. Phagocytosis of OT-55 treated cell by macrophage

K562, KBM-5, KBM-5-T315i and K562R were stained with Cell tracker red (CMTPX) (Thermofisher Scientific) for 1.5 h. After staining, cells were re-suspended in fresh RPMI medium, treated with 30 µM of OT-55 and incubated for 48 h. J774A1 cells were stained with Cell tracker green (CMFDA) (Thermofisher Scientific) for 2 h and allowed to attach to the plate. OT-55-treated CML cells were co-cultured with J774A1 for 2 h with an effector:target ratio of 2:1. Phagocytosis was quantified by measuring the number of double positive cells. To further confirm the level of phagocytosis, CML cells not taken up by J774A1 were removed from the top and level of phagocytosis was quantified by measuring the number of double positive cells.

2.13. Detection of cancer stem cells

For detection of stemness of K562 and K562R cells, 1 x 106 cells were collected, and ALDH activity was determined using Aldefluor kit (STEMCELL Technologies) according to the manufacturer's instructions. To determine the effect of OT-55, omacetaxine alone or in combination, K562R

cells were treated at indicated concentrations and ALDH activity was determined after 72 h of treatment by flow cytometry.

2.14. Measurement of mitochondrial metabolic activity

Seahorse XFp analyzer (Agilent) was used to determine the mitochondrial metabolic activity of CML and ALDH high CML cells. Experiments were performed according to manufacturer's instructions.

2.15. *In vivo* toxicity assay

CD1 mice were obtained from Orient Bio (Seoul, South Korea) and maintained according to SNU guidelines. For acute toxicity assays, mice were daily injected intravenously at indicated concentrations of OT-55 dissolved in ethanol:DMSO at a 1:1 ratio. Body weight was recorded. For chronic toxicity, mice were intravenously injected once at the highest concentration of 80 mg/kg and body weight was recorded for 14 days.

2.16. Zebrafish xenograft assay

For cancer xenograft assays, after mating, fertilized eggs were incubated in Danieau's solution with 0.003% of phenylthiourea (PTU) at 28.5 °C for 48 h. Micropipettes for injection and anesthesia were generated from a 1.0 mm glass capillary (World Precision Instruments, FL, USA) by using a micropipette puller (Shutter Instrument, USA). 48 h post fertilization (hpf), zebrafish were

anesthetized in 0.02 % tricaine (Sigma, MO) and immobilized on an agar plate. K562R cells or primary blasts were treated with indicated compounds for 10 h; then cells were stained for additional 2 h with 4 μM of cell tracker CM-Dil dye (Invitrogen). 100–200 of K562R cells or primary blasts were injected into the yolk sac by microinjection (PV820 microinjector, World Precision Instruments, FL, USA). Subsequently, zebrafish were incubated in 24-well plates containing Danieau's solution with 0.003% phenylthiourea (PTU) at 28.5 °C for 72 h. Fishes were then immobilized in a drop of 3% methylcellulose in Danieau's solution on a glass slide. Pictures were taken by fluorescence microscopy (Leica DE/DM 5000B). Fluorescent tumors were quantified by Image J software (U.S. National Institute of Health, Bethesda, MD, USA).

2.17. Transmission electron microscopy (TEM)

Cells were pelleted and fixed in 2.5% glutaraldehyde (Electron Microscopy Sciences, U.S.A) diluted in 0.1 M sodium cacodylate buffer, pH 7.2 (Electron Microscopy Sciences, U.S.A) overnight. Cells were then rinsed with sodium cacodylate buffer twice and post-fixed in 2% osmium tetroxide for 2 h at room temperature. Samples were washed with distilled water and then stained with 0.5% uranyl acetate in 4 °C for overnight. After 24 h, samples were dehydrated through a graded series of ethanol solutions to water followed by propylene oxide, and then infiltrated in 1:1 propylene oxide/Spurr’s resin. Samples were

kept overnight embedded in Spurr's resin, mounted in molds and left to polymerize in an oven at 56 °C for 48 h. Ultrathin sections (70–90 nm) were obtained with ultramicrotome, EM UC7 (Leica, Germany). Sections were stained with uranyl acetate and lead citrate and subsequently examined with a JEM1010 transmission electron microscope (JEOL, Japan).

2.18. Statistical analysis and bioinformatics

Data are expressed as the mean ± s.d. and significance was estimated by using one-way or two-way ANOVA tests using Prism 6 software, GraphPad Software (La Jolla, CA, USA). P-values <0.05 were considered as significant. Combination index (CI) was calculated according to Chou and Talalay using Compusyn Software (ComboSyn, Inc., Paramus, NJ, USA). CI values below 1 indicate synergism. KEGG pathway was drawn using CyKEGGParser app in Cytoscape software. Color nodes were adapted to represent treatment effect.

3. Results

3.1. OT-55 inhibits the proliferation and viability of imatinib-sensitive or -resistant CML cell lines.

The in vitro effects of OT-55 on cell proliferation and viability were investigated in a panel of CML cell lines, including wild-type imatinib-sensitive and imatinib-resistant cells. Viability/proliferation was assessed at different time-points. OT-55 inhibited CML cell proliferation and viability in a concentration- and time-dependent manner.

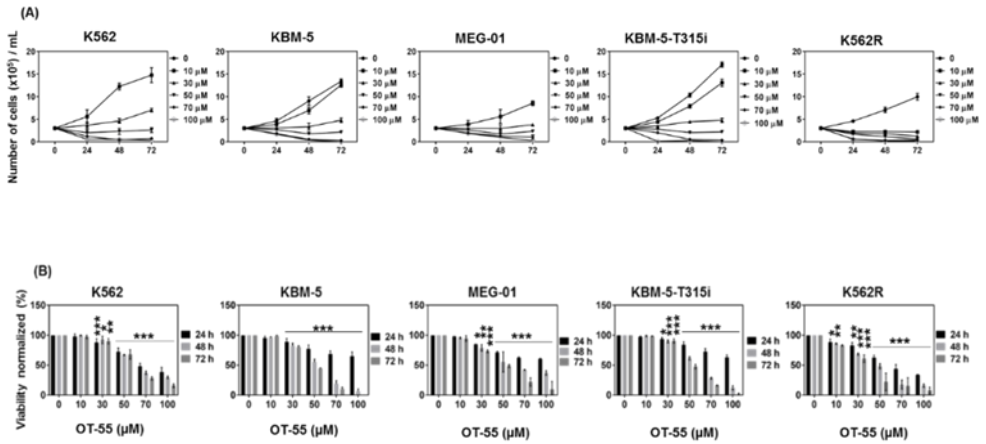

Figure 2. 1: Anti-proliferative and cytotoxicity of OT-55 in CML cell lines.

K562, KBM-5, MEG-01, KBM-5-T315i and K562R cells were treated with the indicated concentrations of OT-55 for 24, 48, or 72 h. (A) Proliferation. (B) Viability. Results correspond to the mean ± SD of three independent experiments.

3.2. OT-55 shows differential toxicity in healthy PBMCs and no acute and chronic toxicity in mice.

The differential toxicity of OT-55 was also investigated ex vivo and in vivo. PBMCs from healthy donors were treated with increasing concentrations of OT-55 and viability was measured. Exposure to the highest concentrations of OT-55 for 48 h reduced viability by 20 to 50% (Fig 2.2 A). To further assess toxicity in vivo, CD1 mice were injected intravenously with various concentrations of OT-55 daily for 7 days. No acute toxicity or reduction in body weight was observed (Fig 2.2 B). Moreover, no chronic toxicity or decrease in body weight was observed in mice that were intravenously injected once with the highest concentration (80 mg/kg OT-55) and observed for 14 days (Fig 2.2 C).

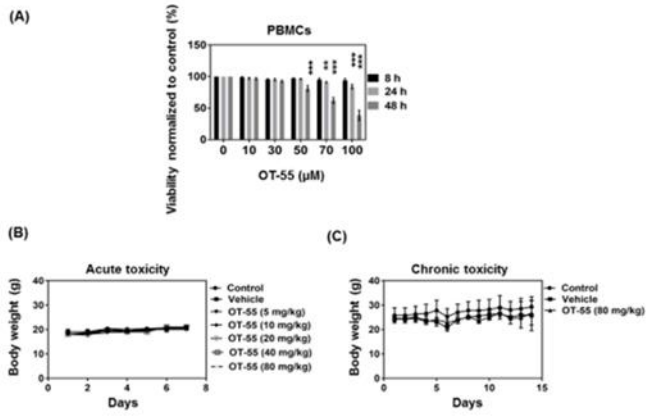

Figure 2. 2: OT-55 exhibit differential toxicity in healthy PBMCs and no acute or chronic toxicity in mice.

PBMCs were treated with indicated concentration of OT-55 for 8, 24 and 48 h (A) differential toxicity. Results correspond to the mean ± SD of three independent experiments. CD1 mice were treated daily with the indicated dose of OT-55 for one week (B) acute toxicity. Four CD1 mice per group were treated with 80 mg/kg OT-55 and observed for two weeks (C) chronic toxicity.

3.3. OT-55 inhibits CML cell cycle and colony formation, and induces apoptosis.

Analysis of DNA content by flow cytometry showed OT-55 concentration-dependent accumulation of cells in G1 phase; this was already detectable after 12 h, and was significant after 24 h (Fig 2.3 A). OT-55-induced cell death was investigated at different time-points. OT-55 produced a concentration-dependent increase in nuclear fragmentation, indicating apoptotic cell death. Moreover, inhibition of OT-55-induced apoptosis in CML by zVad

pretreatment suggested that this was caspase-dependent apoptosis (Fig 2.3 B). K562 cells exposed to 75 µM OT-55 showed a significant decrease in the total number of colonies and from 50 µM showed significant decrease in average size of colonies (Fig 2.3 C).

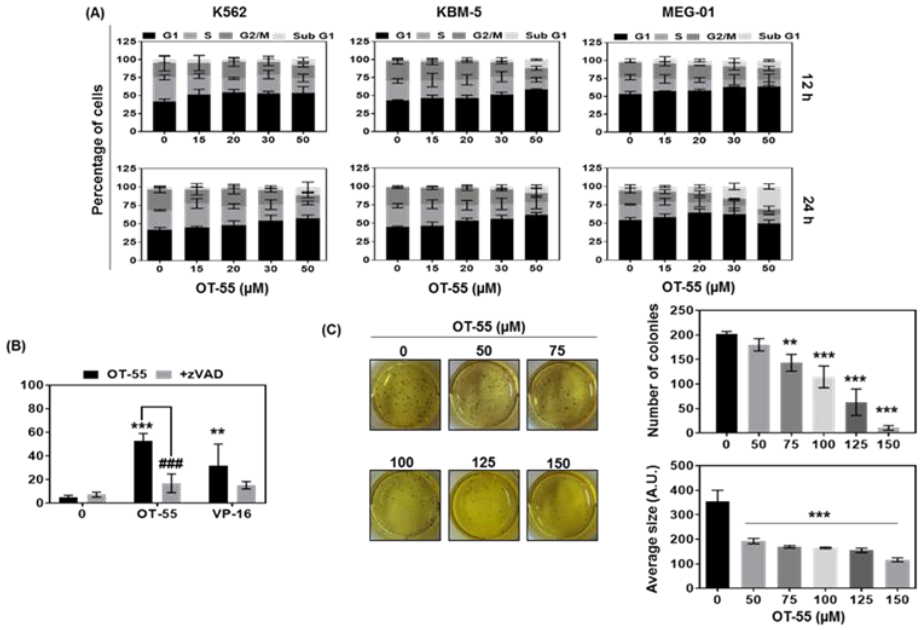

Figure 2. 3: Effect of OT-55 on CML cell cycle, apoptosis, and colony formation.

Cells were treated with the indicated concentrations of OT-55 for 12 h or 24 h. (A) Cells were stained with PI, and DNA content was measured by flow cytometry to estimate cell cycle distribution. (B) Annexin V/PI staining of cells exposed to OT-55 (100 µM) or VP-16 (100 µM) for 24 h, with or without pretreatment with zVad. **p < 0.01, ***p < 0.005 for the comparison of OT-55 treated and untreated cells; ###p < 0.005 for the comparison of cells treated with OT-55, with and without zVad pretreatment. (C) K562 cells were treated with the indicated concentrations of OT-55 and incubated for 10 days to form

colonies. Histograms correspond to the mean ± SD of three independent experiments; *p < 0.05, **p < 0.01, ***p < 0.005 versus untreated cells, respectively.

3.4. OT-55 induces ER stress response in CML.

Next, we evaluated the capacity of OT-55 to trigger ER stress response in CML. OT-55-treated K562 cells showed an ER stress response characterized by phosphorylation of eukaryotic initiation factor 2α and increased expression of activating transcription factor-4 and CCAAT/enhancer-binding protein homologous protein.

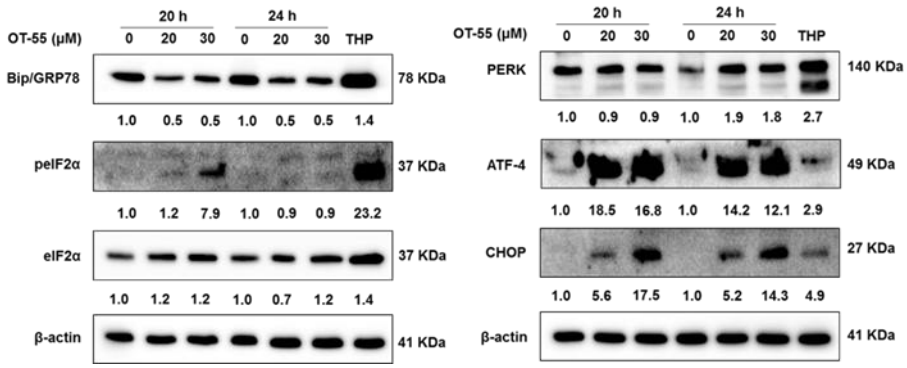

Figure 2. 4: Western blotting of ER stress-related proteins.

K562 cells were treated with the indicated concentrations of OT-55 or with thapsigargin (THP) (500 nM) for 24 h. Blots are representative of three independent experiments.

3.5. OT-55 induces ectopic-calreticulin, ectopic ERp57 and HMGB1 release in CML.

OT-55-treated K562 cells showed ectopic expression of calreticulin and ER-associated protein disulfide isomerase (ERp57), hallmarks of ICD, suggesting initiation of ICD. Moreover, significant release of high mobility group box 1 (HMGB1) into media conditioned by OT-55-treated cells confirmed the induction of ICD; this was observed in both imatinib-sensitive (52.9% increase) and -resistant (24.0% increase) K562 cells.

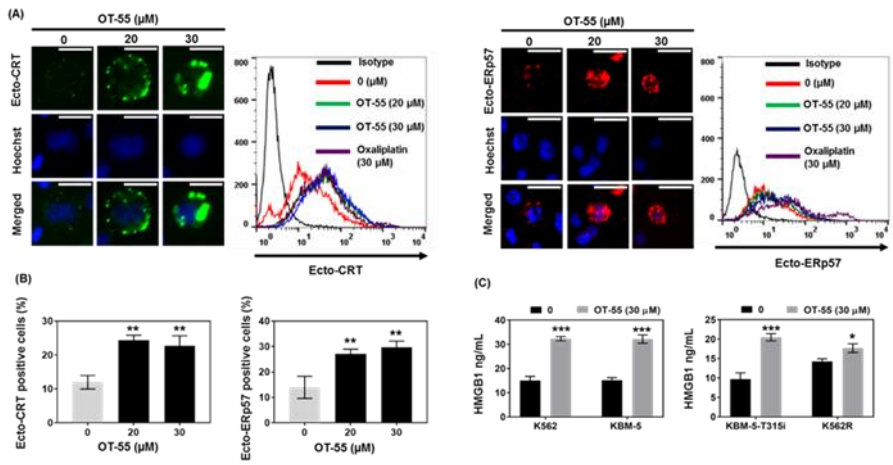

Figure 2. 5: OT-55 triggers ICD in CML and imatinib-resistant CML.

(A) Ectopic expression of calreticulin and ERp57. K562 cells were treated with the indicated concentrations of OT-55 for 24 h. Fluorescence microscopy and facs analysis identified ectopic expression of calreticulin and ERp57. (B) Quantification of ecto-CRT and ecto-ERp57 positive cells. Histograms correspond to the mean ± SD of the quantification of three independent experiments; **p < 0.01. (C) HMGB1 release after a 24 h treatment with OT-

55 (30 µM). Results correspond to the mean ± SD of three independent experiments; *p < 0.05, ***p < 0.005. Scale bars: 50 µm.

3.6. OT-55 promotes phagocytosis of imatinib-sensitive and -resistant CML.

We then assessed whether OT-55 rendered dying cells more susceptible to phagocytosis by macrophages. Red fluorescent K562 cells treated with 30 µM OT-55 for 48 h were co-incubated with green fluorescent J774A1 macrophage cells. Fluorescence microscopy analysis showed stronger interactions between J774A1 cells and OT-55-treated K562 cells, as compared to untreated controls (Figure 2.6 A). Indeed, phagocytosis was initiated after 1 h and was pronounced after 2 h of co-culture (Figure 2.6 B). Our results showed that K562 (33.3%), KBM-5 (40.6%), KBM-5-T315I (30.6%), and K562R (23.3%) cells showed double-positivity, indicating the activation of phagocytosis. As a control, KBM-5-T315I cells were treated for 24 h with 30 µM oxaliplatin, a known inducer of ICD; these cells were phagocytosed after 2 h of co-culture with J774A1 (Figure 2.6 C).

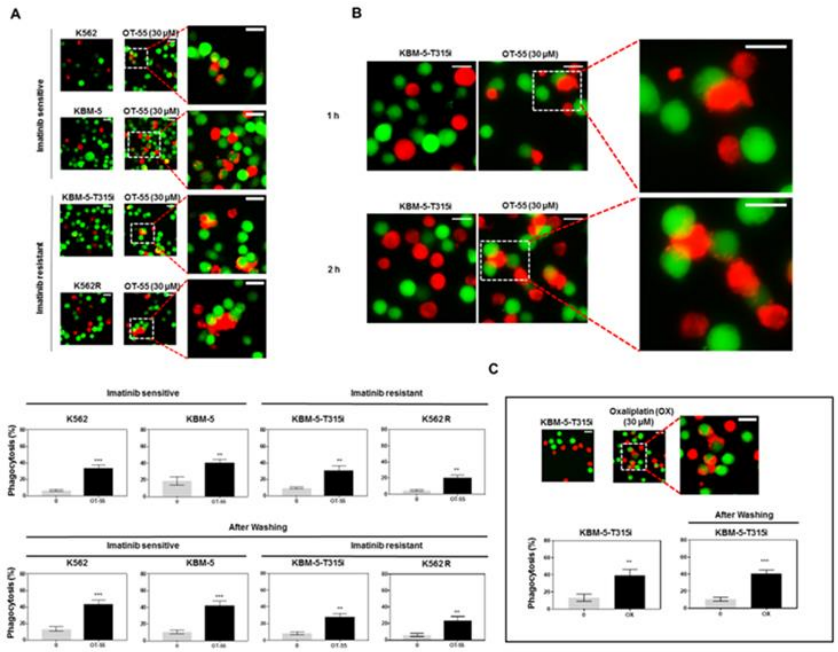

Figure 2. 6: Phagocytosis of OT-55-treated imatinib-sensitive and -resistant cells.

(A) Fluorescence microscopy of K562, KBM-5, KBM-5-T315I, and K562R cells treated with 30 µM OT-55 for 48 h showed phagocytosis by J774A1 macrophages. (B) Fluorescence microscopy of KBM-5-T315I cells treated with 30 µM OT-55 for 48 h and co-cultured with J774A1 macrophages for 1 h and 2 h. (C) KBM-5-T315I cells were treated with 30 µM of oxaliplatin for 24 h. Microscopy images of phagocytosis Quantification of phagocytosis. Histograms correspond to the mean ± SD of three independent experiments; $^{**}p < 0.01$, $^{***}p < 0.005$ versus untreated cells. Scale bars: 20 µm.

3.7. OT-55 shows synergistic cytotoxicity in combination with imatinib.

We investigated the additive or synergistic anti-cancer effects of OT-55 plus imatinib and identified strong induction of nuclear fragmentation (Fig 2.7 A). We determined the Chou-Talalay combination index (CI) in K562 (0.75), KBM-5 (0.77), and MEG-01 (0.75) cells; these values indicated moderate synergistic induction of cell death. Moreover, this combination significantly inhibited colony formation by about 80% in three CML cell lines (Fig 2.7 B).

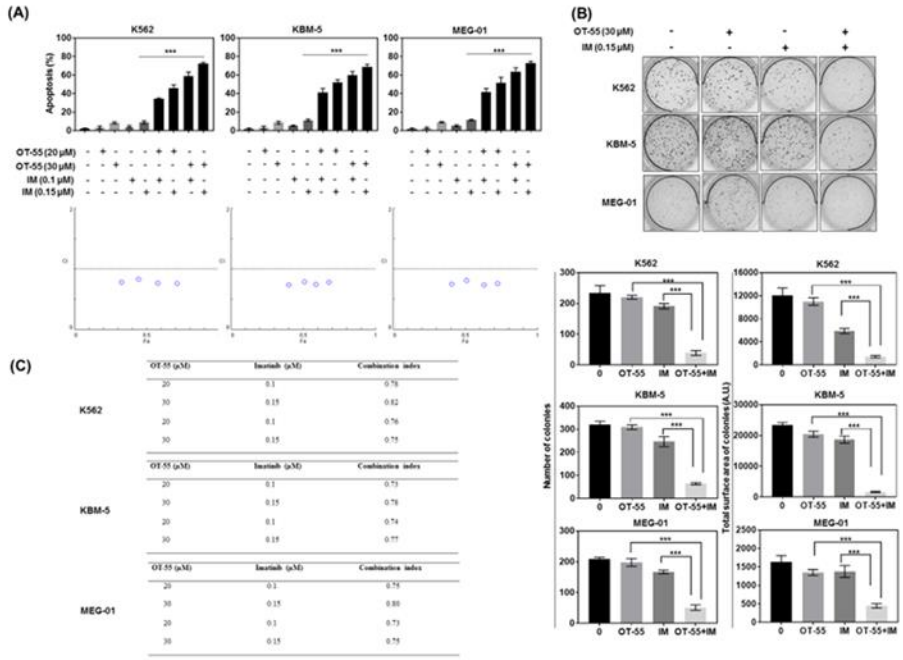

Figure 2. 7: OT-55 plus imatinib produced synergistic cytotoxicity in CML cell lines.

K562, KBM-5 and MEG-01 cells were treated with the indicated concentrations of OT-55, imatinib (IM), or OT-55 plus IM. (A) Apoptosis (percentage of cells) after 24 h. Results correspond to the mean ± SD of three independent experiments; ***$p < 0.005$ for the comparison of the individual and combination treatments. (B) Colony formation in the presence of the indicated concentrations of OT-55, imatinib (IM), or OT-55 plus IM. Results correspond to the mean ± SD of three independent experiments; ***$p < 0.005$. (C) Combination index of OT-55 and imatinib in K562, KBM-5 and MEG-01.

3.8. OT-55 and imatinib combination show mitochondrial damage and onset of apoptosis.

K562 cells were treated with OT-55 (30 µM), imatinib (0.15 µM) or OT-55 and imatinib combination for 6h and 12 h. Transmission electron microscopy was carried out which showed mitochondrial damage at 6 h and 12 h (Fig 2.8 A). The combination didn't show an effect on inhibition of anti-apoptotic proteins Mcl-1 and Bcl-xL. However, cleavage of pro-caspases-9 and -3 after 12 h of this combination treatment confirmed the induction of apoptosis (Fig 2.8 B).

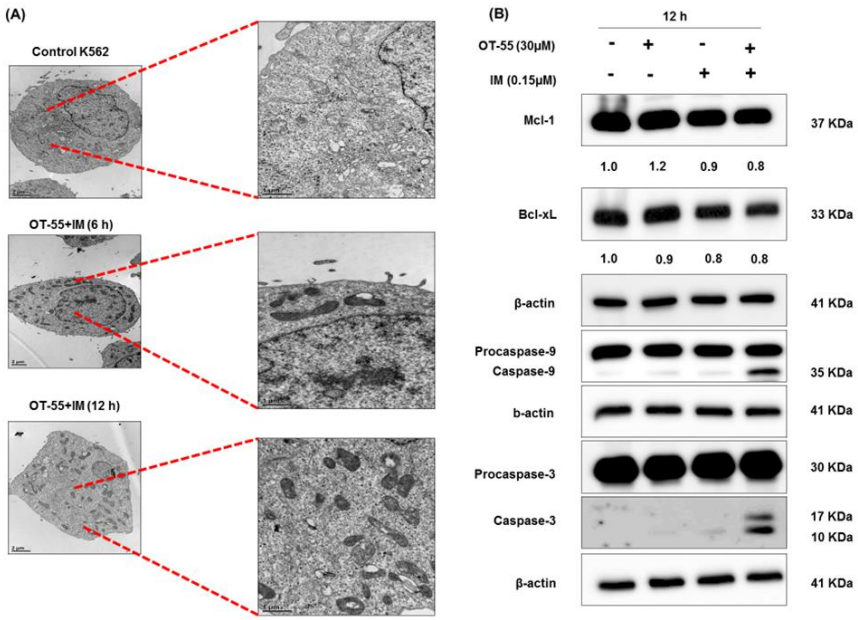

Figure 2. 8: OT-55 and imatinib damage mitochondria and trigger apoptosis.

(A) Transmission electron microscopy pictures of damaged mitochondria. (B) K562 cells were treated with indicated concentration of OT-55 and imatinib. Western blot analysis shows effect of combination on Mcl-1, Bcl-xL, caspase-3 and caspase-9. IM (imatinib).

3.9. OT-55 and imatinib abrogate tumor formation in zebrafish xenograft assay.

Human primary cells were treated with OT-55 (30 µM), imatinib (0.15 µM) or OT-55 and imatinib combination for 12 h. Treated cells were injected into the zebrafish yolk sac. After 72 h of incubation, tumor formation was monitored by measuring the fluorescence integrated density. OT-55 (30 µM)

and imatinib (0.15 µM) individually reduced tumor formation. However, the combination completely abrogated the tumor formation in the zebrafish yolk sac.

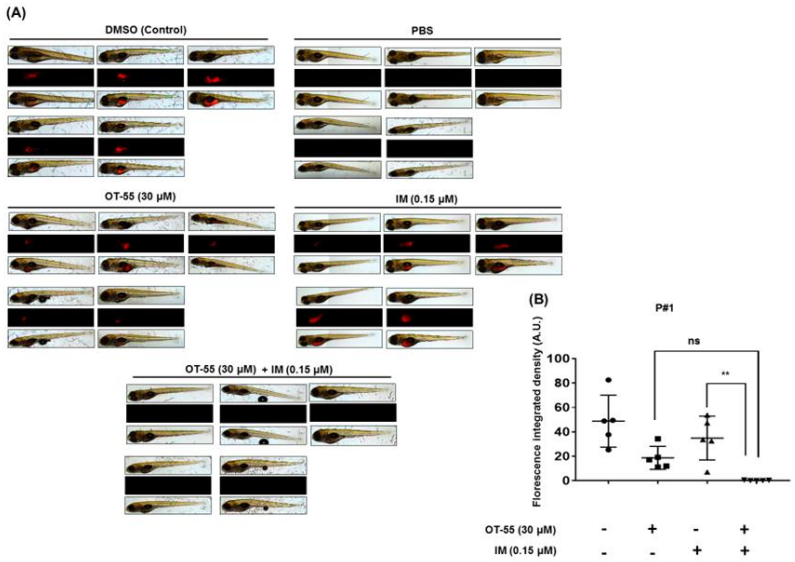

Figure 2. 9: Zebrafish Xenograft assay with human primary samples.

(A) Pictures of tumor formation in the zebrafish yolk sac. (B) Quantification of fluorescence integrated density. ns non-significant, **p < 0.01. IM (imatinib).

3.10. OT-55 inhibits tumor necrosis factor α (TNFα)-induced NF-κB activation in K562 cells.

Bcr-Abl activates NF-κB signaling in CML, and we therefore investigated this pathway by CyKEGGParser, confirming the activation of STAT5 (Fig 2.10 A). We found that imatinib plus OT-55 inhibited the phosphorylation of Bcr-Abl by 100% and of STAT5 by 90% after a 2 h treatment. We further confirmed that OT-55 inhibited TNFα-induced NF-κB activation, with a half-maximal inhibitory concentration of 4.4 ± 2.0 μM. The NF-κB inhibitor, goniothalamin, served as a positive control. Concentration-dependent inhibition of the expression of an NF-κB target gene, intercellular adhesion molecule 1 (ICAM-1) was also observed with a half-maximal inhibitory concentration of 2.0 ± 2.0 μM; this confirmed the involvement of NF-κB signaling in OT55-mediated induction of cell death (Fig 2.10 B).

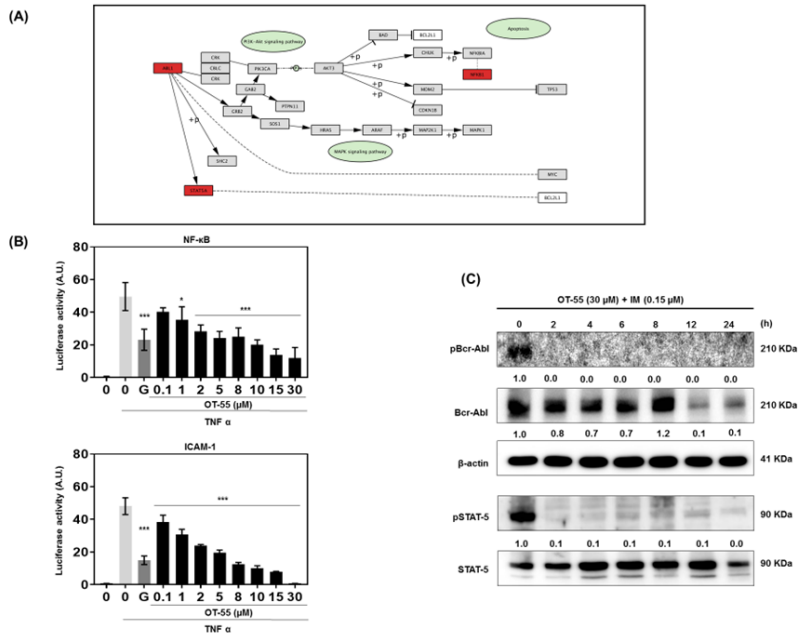

Figure 2. 10: OT-55 inhibits TNFα-induced NF-κB activation in K562 cells.

(A) Bcr-Abl activation of NF-κB signaling in CML is impaired by the indicated treatments. The ABL part of the CML KEGG pathway is represented. Colors: inhibition (red), no effect (white), default (grey). Green circles represent the main pathway subgroups. Bcl-xL is annotated as BCL2L1. (B) NF-κB and ICAM-1 luciferase activity after 8 h treatments with the indicated concentrations of OT-55 or 7 μM goniothalamin (G). Results correspond to the mean ± SD of three independent experiments; **p < 0.01, ***p < 0.005. (C) Expression of pBcr-Abl, Bcr-Abl, pSTAT5, and total STAT5 in K562 exposed to OT-55 plus imatinib (IM) for the indicated time periods.

3.11. OT-55 shows synergistic cytotoxicity in combination with omacetaxine on KBM-5-T315I and K562R cells.

In order to validate the synergistic potential of OT-55 on imatinib-resistant CML, we used OT-55 plus omacetaxine on imatinib-resistant KBM-5-T315I and K562R cells. Analysis of nuclear morphology showed a synergistic induction of apoptosis in cells exposed to OT-55 plus omacetaxine for 24 h (Fig 2.11 A) (CI = 0.62). This combination treatment reduced the expression level of myeloid cell leukemia 1 (Mcl-1) by 70% after 2 h, and by 90% after 12 h, without affecting the expression of B-cell lymphoma 2 (Bcl-2) or Bcl-extra large (Bcl-xL) (Fig 2.11 B). These results indicated that the early decrease in Mcl-1 could cause the induction of apoptosis by this combination treatment. OT-55 alone did not alter the expression of Mcl-1, whereas omacetaxine reduced its expression by 90% after a 12-h treatment. However, Mcl-1 expression had recovered to 40% of the control level after 24 h. Interestingly, in KBM-5 cells, OT-55 plus imatinib did not alter the expression of Bcl-2, Bcl-xL, or Mcl-1 (Fig 2.11 B). In K562R cells, Hoechst/propidium iodide (PI) staining followed by fluorescence microscopy showed that 60% of the cells were PI-positive, suggesting necrosis as a main cell death mechanism (Fig 2.11 A). Furthermore, western blot analysis showed 100% inhibition of Mcl-1 after a 2 h treatment. However, Mcl-1 expression recovered to 30% after 6 h, to 60% after 12 h, and was strongly overexpressed (140%) at 24 h

(Fig 2.11 C). Mcl-1 expression levels were similar in K562 and K562R cells, and OT-55 plus imatinib did not alter the expression of Mcl-1.

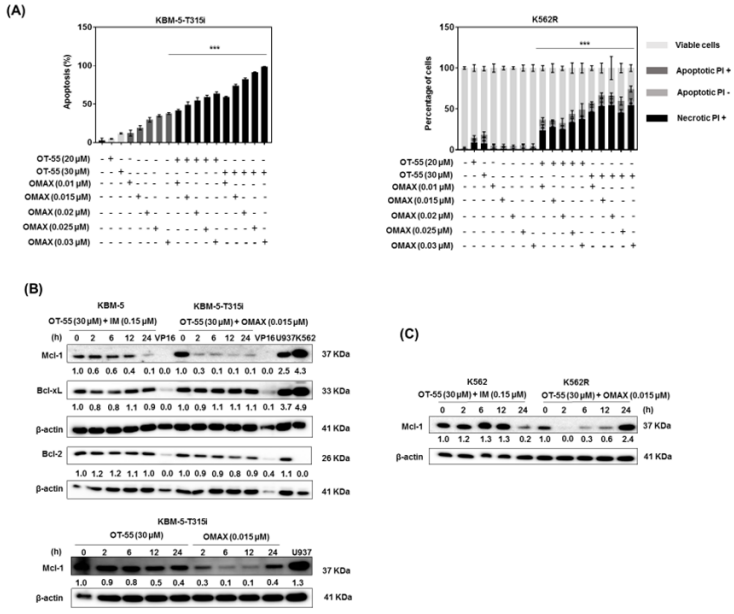

Figure 2. 11: OT-55 plus omacetaxine produced synergistic cytotoxicity in KBM-5-T315I and K562R cells.

(A) The level of apoptosis or cell death (percentage) was quantified in KBM-5-T315i and K562R cells. Results correspond to the mean ± SD of three independent experiments. (B) Expression of Mcl-1, Bcl-xL, and Bcl-2 in KBM-5 and KBM-5-T315I cells exposed to the indicated treatments or VP-16 (50 µM) for 10 h, and untreated U937 and K562 cells. Expression of Mcl-1 in KBM-5-T315I cells exposed to OT-55 (30 µM) or omacetaxine (OMAX) (0.015 µM) for the indicated time-periods, and in untreated U937 cells. (C) Expression of Mcl-1 and Bcl-xL in K562 and K562R cells exposed to the indicated treatments, and in untreated U937 cells.

3.12. OT-55 inhibits ALDH positive cells and mitochondrial oxidative metabolism of ALDH high K562R cells.

Imatinib-resistant K562R cells showed a greater sub-population of highly ALDH-positive cells than did K562 cells (+29.3%). OT-55 treatment for 72 h strongly reduced the number of ALDH-positive cells; this effect was not potentiated by combination treatment with omacetaxine (Fig 2.12 A, B). We next compared the mitochondrial oxidative metabolism profiles in K562 cells and ALDH-positive K562R cells. Imatinib-resistant K562R cells showed a 51.9% increase in their ATP-linked mitochondrial oxygen consumption rate (OCR) and a 42.2% increase in their maximal OCR. OT-55 treatment of imatinib-resistant K562R cells reduced the basal OCR by 15.3%, increased the ATP-linked OCR by 82.2%, and decreased the maximal OCR by 56.7%. The increase in ATP-linked OCR after OT-55 treatment suggested an increased ATP requirement as a consequence of cellular stress (Fig 2.12 C, D).

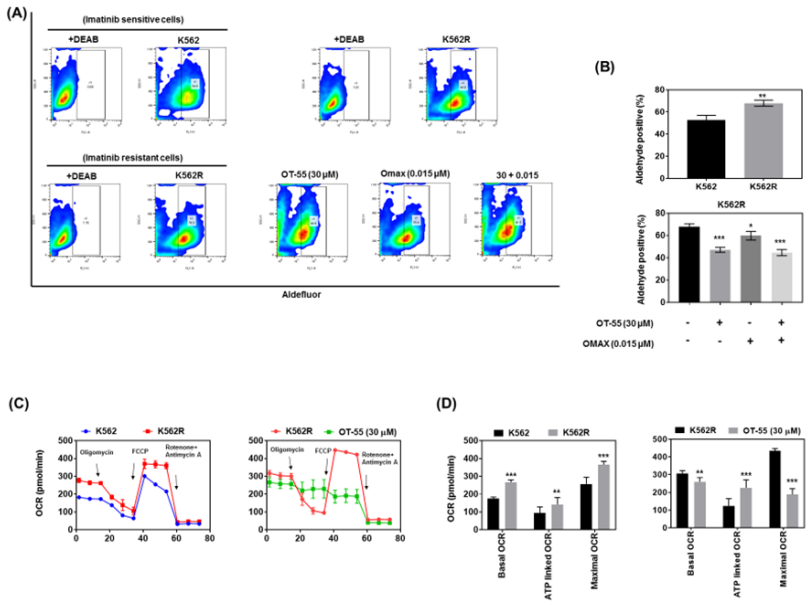

Figure 2. 12: OT-55 inhibits ALDH positive cells and mitochondrial oxygen consumption rate in K562 R cells.

(A) Facs analysis of ALDH positive cells in K562 and K562R cells. (B) Quantification of ALDH activity in K562 and K562R cells treated for 72 h with OT-55 (30 µM), omacetaxine (0.015 µM) or OT-55 (30 µM) plus omacetaxine (0.015 µM). Results correspond to the mean ± SD of three independent experiments. *p < 0.05, **p < 0.01, ***p < 0.005 versus untreated cells, respectively. (C) Mitochondrial respiration in K562 and K562R cells by sea horse analysis. (D) Quantification of mitochondrial oxygen consumption rate in K562 and K562R cells and K562R cells treated with OT-55 for 48 h. Results correspond to the mean ± SD of three independent experiments; **p < 0.01, ***p <0.005 versus untreated cells.

3.13. OT-55 and omacetaxine abrogate tumor formation of K562 R cells in zebrafish xenograft assay.

To extend our results to an in vivo situation, we injected imatinib-resistant K562R cells that had been pre-treated with OT-55 (30 µM) and omacetaxine (0.015 µM) into zebrafish. These results showed that the combination pretreatment completely inhibited tumor formation and produced a greater effect than the individual treatments.

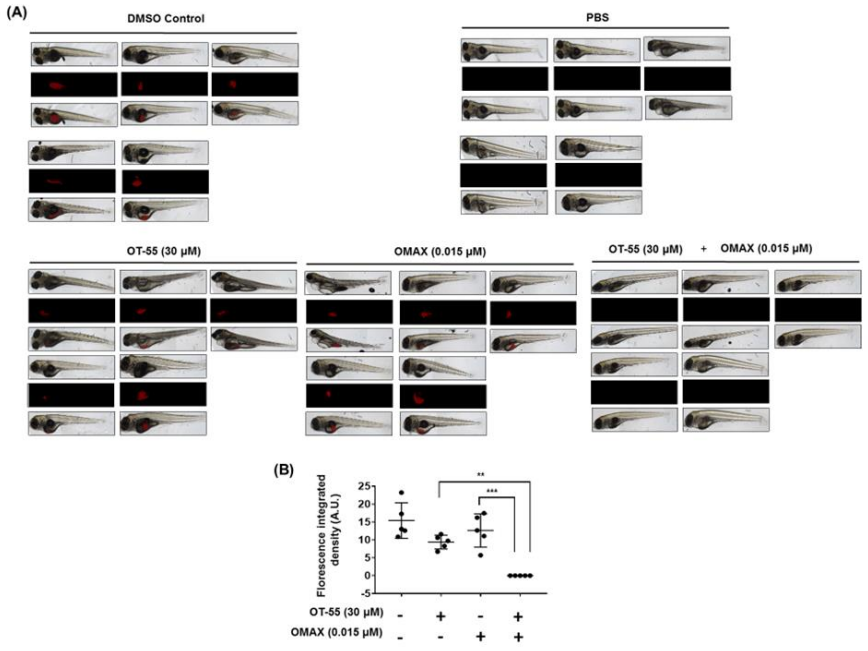

Figure 2. 13: OT-55 and omacetaxine inhibit K562R cells tumor formation in zebrafish yolk sac.

(A) Pictures of tumor formation in the zebrafish yolk sac. (B) Quantification of fluorescence integrated density. ns non-significant, **p < 0.01, *** p < 0.005. Omax (Omacetaxine).

4. Discussion

TKIs provide a targeted therapeutic approach for CML, but imatinib resistance due to the acquisition of T315I mutation and the existence of CML stem cells pose challenges for a relapse-free clinical remission of the disease. In the present study, we demonstrated that OT-55, a biscoumarin derivative, inhibited cell proliferation, induced cell death, and produced synergistic cytotoxicity in combination with imatinib or omacetaxine in models of imatinib-sensitive or -resistant CML.

Moreover, we investigated the capacity of OT-55 to induce ICD in both imatinib-sensitive and resistant cell lines. We report here for the first time that a biscoumarin induced ICD in CML. Surface exposure of calreticulin and ERp57, and the release of HMGB1, provide markers of the ability of a compound to induce ICD. These act as "eat me" or "kill me" signals by a dying cancer cell, to attract dendritic or natural killer cells [30]. OT-55 treatment produced strong ectopic expression of calreticulin. Furthermore, the release of HMGB1 confirmed ICD in both imatinib-sensitive and resistant CML. Cyclophosphamide, an alkylating agent that is employed to treat various hematological malignancies including CML, is known to trigger an immunomodulatory response by mechanisms involving the inhibition of tumor-induced suppressor T-cells, activation of long-term survival,

proliferation of lymphocytes, and production of several soluble mediators [31]. Imatinib was also shown to trigger natural killer cell function in mice and humans. However, the present study has provided the first report of ICD induction in cells harboring T315I mutation [32].

Moreover, we demonstrated that OT-55 triggered synergistic cytotoxicity of CML cells in combination with imatinib at a concentration range of 100 150 nM. STAT5 phosphorylation was reduced after a 2 h treatment, confirming that this combination acted downstream of the Bcr-Abl pathway. STAT transcription factors are constitutively activated both by mutant tyrosine kinases and other pathogenic events, and are involved in mediating the effects of cytokines in myeloid cells [33]. Moreover, STAT5 production is activated by Bcr-Abl signaling during the process of disease progression [34]. Recently, it was reported that the inhibition of STAT5 by a combination of imatinib and the peroxisome proliferator-activated receptor γ agonist, pioglitazone, eradicated CML stem cells [35].

In CML, Bcr-Abl is known to activate NF-κB signaling [36]. OT-55 inhibited TNFα-induced NF-κB signaling and reduced expression of the NF-κB target gene, ICAM-1. These findings confirmed that OT-55 acted downstream of the Bcr-Abl pathway and potentiated the activity of imatinib. Previously, we reported that bis(4-hydroxy-2H-chromen-2-one), a coumarin compound, inhibited NF-κB, leading to cell cycle arrest and apoptosis in leukemia [29].

We further investigated the efficacy of OT-55 in combination with omacetaxine, which is approved for patients with the T315I mutation and is known to act against CML stem cells [37]. In KBM-5-T315I mutant cells, inhibition of Mcl-1 was observed after 2 h of this combination treatment, followed by apoptosis. The combination produced synergistic cytotoxicity in KBM-5-T315I cells. Inhibition of Mcl-1 and the induction of apoptosis by omacetaxine treatment alone at concentrations ranging from 10 100 nM has previously been reported in CML [38]. Our results indicated that although 15 nM of omacetaxine alone inhibited Mcl-1 at 2 h, its expression level had increased at 24 h; this indicated that the combination treatment produced a synergistic downregulation of Mcl-1, which ultimately triggered apoptosis. Although the expression level of Mcl-1 was comparable in KBM-5 and KBM-5-T315I cells, its inhibition and subsequent apoptosis suggested that targeting anti-apoptotic Bcl-2 family proteins with additional BH-3 mimetics such as venetoclax or navitoclax could be useful in imatinib-resistant CML. A recent study showed that a combination of venetoclax with TKIs produced strongly synergistic effects on Bcr-Abl-positive acute lymphoblastic leukemia [39] .

We investigated the efficacy of omacetaxine in combination with OT-55 in K562R cells that showed increased ALDH activity and increased mitochondrial OCR. Increased ALDH activity acts as a stem cell marker in hematopoietic and solid tumors [40]. A 72-h treatment of K562R cells with

OT-55 strongly inhibited ALDH activity, suggesting that this compound targeted CML stem cells. A recent study indicated that CML stem cells maintained an upregulated level of mitochondrial oxidative phosphorylation. Targeting oxidative metabolism thus selectively eradicates CML stem cells [41]. Our results were in line with this finding, since ALDH-positive cells showed an increased rate of oxidative metabolism, which was inhibited by OT-55. This suggests that OT-55-mediated inhibition of mitochondrial function could produce therapeutic benefits by targeting CML stem cells. Moreover, our observation of Mcl-1 re-expression after a 24-h treatment of K562R cells, in the absence of apoptosis, confirmed that Mcl-1 is a key target protein in CML stem cells. Interestingly, combination treatment-mediated induction of necrosis suggested that an alternative cell death pathway can be activated in CML stem cells.

Citrus fruits rich in coumarin derivatives may interfere with the metabolism of these compounds in the liver.27 In particular, grapefruit furanocoumarins affect the activity of cytochrome 3A4, a phase I detoxification enzyme [42]. As a consequence, serum drug levels increase and this can lead to severe side effects. Further investigations should be conducted to determine whether the present OT-55 coumarin derivative also interferes with detoxification mechanisms, and precautions should be taken when using this compound in combination with other drugs or foods.

Recent studies demonstrated the efficacy of novel molecules such as farnesyl transferase inhibitors, proteasome inhibitors, histone deacetylase inhibitors, and autophagy inhibitors to overcome tyrosine kinase resistance in CML [43-45]. These approaches clearly evidence an increasing interest in the development of novel compounds to overcome tyrosine kinase resistance in CML. Our study characterized the ICD-inducing, anti-proliferative, pro-apoptotic, and synergistic activities of OT-55, highlighting coumarins as attractive candidates for future lead optimization.

CHAPTER II

HDAC inhibitor martinostat induces immunogenic cell death and synergies with imatinib in imatinib-sensitive and –resistant chronic myeloid leukemia.

1. Purpose of this study

Histones are the most prominent protein of the nucleus and play a major role in modulating the binding of transcription factors to DNA [46]. The activity of histones is tightly regulated by its acetylation status which is regulated by both acetyltransferases and deacetylases. Histone deacetylases are divided into distinct classes: class I (HDAC 1,2,3 and 8), class IIa (HDAC 4,5,7and 9), class IIb (HDAC 6 and 10), class III (sirtuins) and class IV (HDAC 11) [46]. HDAC inhibitors are hydroxamic acids, benzamides, cyclic peptides, ketones or aliphatic acids and each HDAC inhibitor targets different isoforms of HDAC.

In CML, different protein function has been shown to be regulated by the status of acetylation and deacetylation [47]. Moreover, alteration in the acetylation status of non-histone protein can contribute to malignancy and resistance to apoptosis. Imatinib resistance in CML has been linked to concurrent upregulation of class I and class III deacetylases and downregulation of several histone acetyltransferases (HATs) [48]. Additionally, unlike tyrosine kinase inhibitors or chemotherapy, which target dividing cells, HDAC inhibitors can target non-dividing cells which is of advantage to eliminate quiescent CML stem cell pool. Quiescent CML stem cells are a major limiting factor associated with disease relapse and resistance

to tyrosine kinase therapy [35]. Vorinostat (SAHA) treatment in CML restored acetylation pattern of several proteins and altered the apoptotic threshold. Moreover, HDAC inhibitor LBH was shown to effectively target CML stem cells which impaired the tumor forming ability by CML stem cell engraftment in immunodeficient mice [45].

Recent studies have highlighted the role of epigenetics in immune evasion. Epigenetic modulators such as DNA methyltransferase and HDAC inhibitors were able to reverse the immune suppressed tumor microenvironment by mechanisms such as enhancing the expression of tumor associated antigens, component of antigen processing and presenting machinery pathways, immune checkpoint inhibitors, chemokines, and other immune-related genes [49]. These discoveries allowed us to investigate the anti-cancer effect and immunomodulatory effects of a HDAC inhibitor martinostat in imatinib sensitive and -resistant chronic myeloid leukemia.

2. Material and methods

2.1. Cell culture and treatment

Chronic myeloid leukemia cell lines K562 and MEG-01 were purchased from Deutsche Sammlung für Mikroorganismen und Zellkulturen (DSZM; Braunschweig, Germany) and cultured in RPMI medium (Lonza, Basel, Switzerland) supplemented with 10% (v/v) fetal calf serum (FBS) (Biowest,

Nuaille, France) and 1% (v/v) antibiotic–antimycotic (Lonza, Basel, Switzerland) at 37 °C and 5% of CO2. KBM-5 cells were kindly donated by Dr. Bharat B. Aggarwal and KBM-5. KBM-5-T315i cells were developed by culturing the cells with imatinib. Imatinib concentration was increased eventually from 0.25, 0.5 and finally cultured with 1 μM of in IMDM media supplemented with 10% (v/v) fetal calf serum and 1% (v/v) antibiotic–antimycotic. K562R cells were a gift of the Catholic University, Seoul and cultured in RPMI medium with 25 mM HEPES (Lonza, Basal, Switzerland) supplemented with 10% (v/v) FBS and 1% (v/v) antibiotic-antimycotic. Both resistant cells were cultured with 1 μM of imatinib and washed three times before experiment.

2.2. Cell proliferation and viability

Cell proliferation and viability were measured by using the trypan blue exclusion assay (Lonza, Basel, Switzerland). The number of cells per mL was counted, and the fraction of trypan blue-positive cells was estimated by using a Malassez cell counting chamber (Marienfeld, Lauda-Königshofen, Germany).

2.3. Cell cycle distribution

For cell cycle analysis, cells were collected and fixed in 70% ethanol. DNA was stained with a propidium iodide (PI) solution (1 μg/mL, Sigma-Aldrich,

St. Luis, Missouri, USA) in 1x PBS (Hyclone), supplemented with RNase A (100 μg/mL; Roche, Basel, Switzerland). Samples were analyzed by flow cytometry using a FACS CaliburTM system, Becton Dickinson (BD) Biosciences (FACS) (San Jose, CA, USA). Data were recorded statistically (20,000 events/sample) using the Cell Quest software (BD Biosciences) and analyzed using Flow-Jo 8.8.5 software (Tree Star, Inc., Ashland, OR, USA).

2.4. Protein extraction and western blot

Whole cell extracts were prepared using M-PER® (Thermofisher, Waltham, Massachusetts, USA) supplemented with 1x protease inhibitor cocktail (Complete EDTA-free, Roche, Basel, Switzerland) according to the manufacturer's instructions. Proteins were resolved by SDS-PAGE and transferred to PVDF membranes (GE Healthcare, Little Chalfont, UK). Membranes were incubated with selected primary antibodies (Supplementary Table I). Chemo-luminescence signal was detected with the ECL Plus Western Blotting Detection System (GE Healthcare, Little Chalfont, UK) and quantified by ImageQuant LAS 4000 mini system (GE Healthcare).

2.5. Evaluation of apoptosis

The percentage of apoptotic cells was quantified as the fraction of cells showing fragmented nuclei, as assessed by fluorescence microscopy (Nikon, Tokyo, Japan) after staining with Hoechst 33342 (Sigma-Aldrich) and

propidium iodide (Sigma-Aldrich). Apoptosis was also confirmed by annexin V/propidium iodide staining and fluorescence-activated cell sorter (FACS) analysis according to the manufacturer protocol (BD Biosciences).

2.6. Colony formation assay

For colony formation assays, 103 cells/mL were grown in a semi-solid methylcellulose medium (Methocult H4230, StemCell Technologies Inc., Vancouver, Canada) supplemented with 10% FBS and indicated concentrations. Colonies were detected after 10 days of culture by adding 1 mg/mL of 3-(4,5-dimethylthiazol-2-yl)-2,5-diphenyltetrazolium bromide (MTT) reagent (Sigma) and were scored by Image J 1.8.0 software (U.S. National Institute of Health, Bethesda, MD, USA).

2.7. Analysis of immunogenic cell death markers calreticulin and ectopic expression of ERp57

10^6 cells were cultured and treated at indicated concentrations of OT-55 for 24 h. Cells were collected, washed twice with 1x PBS and fixed in 0.25% paraformaldehyde in 1x PBS for 5 min. After washing again twice in cold PBS, cells were incubated for 30 minutes with the primary antibody for calreticulin or ERp57, diluted in cold blocking buffer (2% FBS in 1x PBS), followed by washing and incubation with the Alexa488-conjugated monoclonal secondary antibody in a blocking buffer (for 30 min). Each sample was then analyzed by

FACS and fluorescence microscopy to identify cell surface CRT or ERp57. Isotype-matched IgG antibodies were used as a control.

2.8. Detection of HMGB1 release

Cells were seeded in 1 mL of medium. After 24 h, cells were centrifuged, the supernatant was collected and immediately stored at -80 ºC. Quantification of HMGB1 release in the supernatants was assessed by enzyme-linked immunosorbent assay kit from Shino-Test-Corporation (Jinbocho, Chiyoda-ku, Tokyo, Japan) according to the manufacturer's instructions.

2.9. Statistical analysis

Data are expressed as the mean ± s.d. and significance was estimated by using one-way or two-way ANOVA tests using Prism 6 software, GraphPad Software (La Jolla, CA, USA). P-values <0.05 were considered as significant. Combination index (CI) was calculated according to Chou and Talalay using Compusyn Software (ComboSyn, Inc., Paramus, NJ, USA). CI values below 1 indicate synergism.

3. Results

3.1. Martinostat inhibits cell proliferation in la ow concentration range compared to vorinostat

The in vitro effects of martinostat and vorinostat on cell proliferation was investigated in a panel of CML cell lines, including wild-type imatinib-sensitive and imatinib-resistant cells. K562, KBM-5, K562R and KBM-5-T315I cells were treated with different concentration of martinostat and vorinostat. Proliferation was assessed at 24, 48 and 72 h. Both martinostat and vorinostat inhibited CML cell proliferation in a concentration- and time-dependent manner. However, martinostat inhibited cell proliferation in concentration range lower than vorinostat.

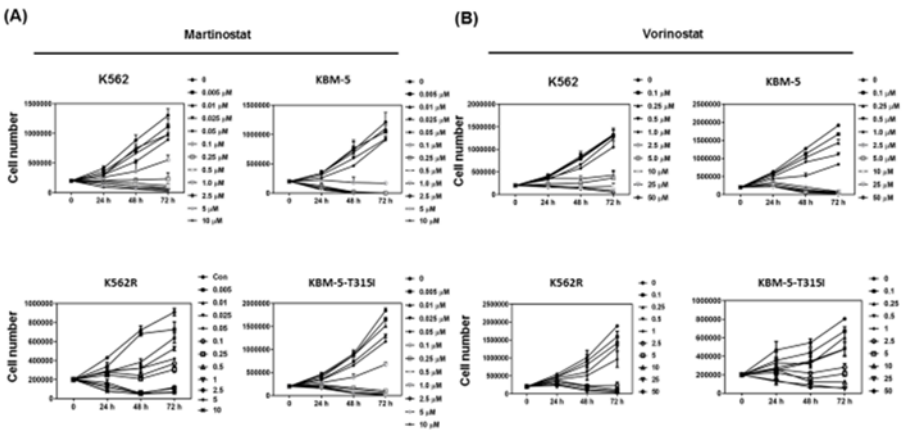

Figure 3. 1: Martinostat and vorinostat inhibit CML cell proliferation.

K562, KBM-5, KBM-5-T315i and K562R cells were treated with the indicated concentrations of martinostat and vorinostat for 24, 48, or 72 h. (A)

inhibition of proliferation by martinostat (B) Inhibition of proliferation by vorinostat. Results correspond to the mean ± SD of three independent experiments.

3.2. Martinostat inhibits CML cell viability in low concentration range compared to vorinostat

The in vitro effect of martinostat and vorinostat on cell viability was investigated in a panel of CML cell lines, including wild-type imatinib-sensitive and imatinib-resistant cells. K562, KBM-5, K562R and KBM-5-T315I cells were treated with different concentration of martinostat and vorinostat. Viability was assessed by trypan blue exclusion assay at time-points 24, 48 and 72 h. Both martinostat and vorinostat inhibited CML cell viability in a concentration- and time-dependent manner. However, martinostat inhibited cell viability in concentration range lower than vorinostat.

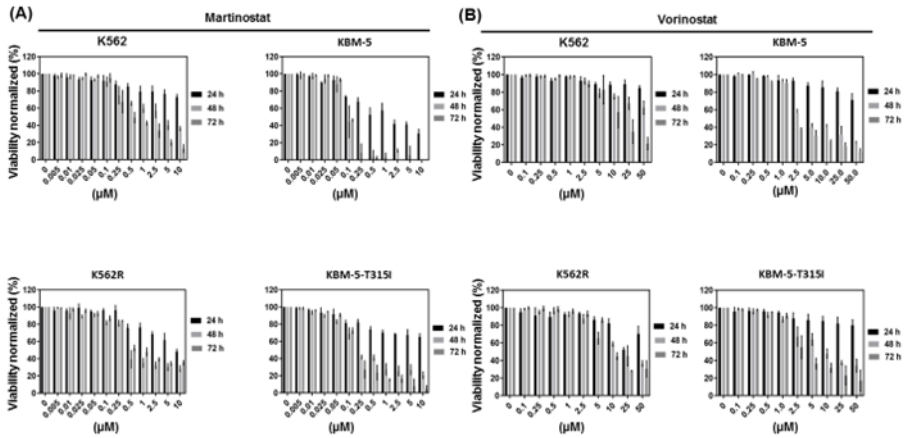

Figure 3. 2: Martinostat and vorinostat inhibits CML cell viability.

K562, KBM-5, KBM-5-T315I and K562R cells were treated with the indicated concentrations of martinostat and vorinostat for 24, 48, or 72 h. (A) inhibition of viability by martinostat (B) Inhibition of viability by vorinostat. Results correspond to the mean ± SD of three independent experiments.

3.3. Martinostat and vorinostat inhibit CML colony formation

In order to investigate the effect of martinostat and vorinostat on anchorage-independent colony formation, K562 cells were treated with different concentrations of martinostat and vorinostat. After 10 days of incubation, martinostat at 0.05 (μM) inhibited more than 80 % of colony formation whereas vorinostat reduced 80 % of colony formation at concentration 10 (μM).

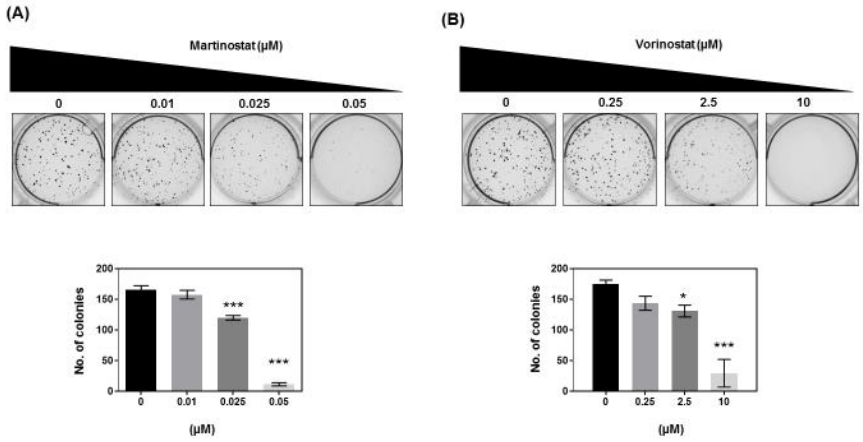

Figure 3. 3: Inhibition of colony formation.

K562 cells were treated with different concentrations of martinostat and vorinostat. (A) Inhibition of colony formation by martinostat. (B) inhibition of colony formation by vorinostat. Results correspond to the mean ± SD of three independent experiments; *p< 0.5, ***p < 0.005.

3.4 . Martinostat inhibits CML cell cycle

Analysis of DNA content by flow cytometry showed martinostat concentration-dependent accumulation of cells in G1 phase; this was already detectable after 12 h, and increased significantly after 24 h. Vorinostat showed accumulation of cells in G1 phase after 24 h of treatment in K562. However, for KBM-5 and MEG-01 it didn't show an increase.

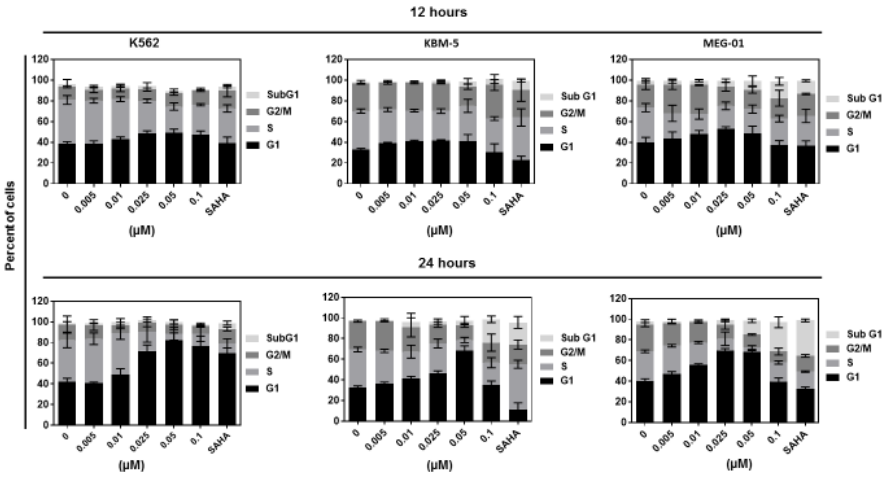

Figure 3. 4: Inhibition of CML cell cycle by martinostat.

K562, KBM-5 and MEG-01 cells were treated with indicated concentration of martinostat of 2 μM of vorinostat (SAHA). Cell cycle was determined after 12 h and 24 h. Results correspond to the mean ± SD of three independent experiments.

3.5. Martinostat showed ectopic expression of calreticulin and ERp57

Next, we wanted to investigate the ICD-inducing ability of martinostat in CML. K562 cells were treated with 0.15 (μM) and 0.25 (μM) of martinostat for 36 h. 2-fold and 2.5-fold increase in ectopic expression of calreticulin and ERp57 was observed suggesting initiation of ICD by martinostat treatment.

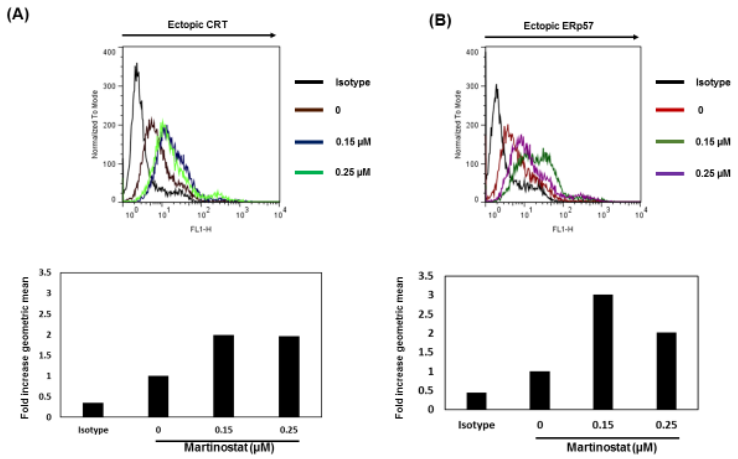

Figure 3. 5: Ectopic expression of calreticulin and ERp57.

K562 cells were treated with indicated concentration of martinostat for 36 h. Ectopic expression of calreticulin and ERp57 was measured by Facs analysis. (A) Ectopic calreticulin. (B) Ectopic ERp57. Histogram represent fold increase in geometric mean.

3.6. Martinostat in combination with imatinib shows caspase dependent apoptosis in CML.

Next, we wanted to investigate the effect of martinostat in combination with imatinib. K562 cells were treated with sub-toxic concentrations of martinostat and imatinib. Annexin V/ PI staining was carried out after 24 h. Combination of martinostat 0.25 (µM) and imatinib (0.1 µM) showed significant increase in Annexin V positive cells compared to individual treatment. Moreover, significant inhibition of annexin V positive cells by pre-zVad treatment

suggested apoptosis is caspase dependent. The combination treatment did not show decrease in the expression of anti-apoptotic protein Bcl-xL. However, Mcl-1 expression was decreased followed by cleavage of caspase 3 and PARP-1.

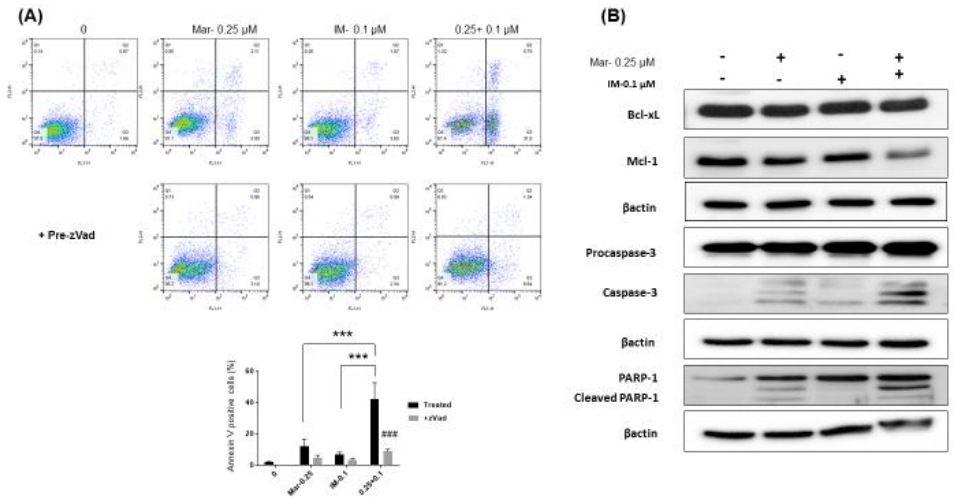

Figure 3. 6: Martinostat potentiates the effect of imatinib in CML.

K562 cells were treated with indicated concentration of martinostat or imatinib or martinostat in combination with imatinib. (A) Annexin V/PI staining after 24 h of treatment with and without pre-zVad treatment. Histogram correspond to the mean ± SD of three independent experiments; ***p < 0.005 significant difference between individual and combination treatment; ###p< 0.005 significant difference between with and without pre-zVad treatment. (B) Western blot for anti-apoptotic proteins Bcl-xL, Mcl-1 and caspase 3 and PARP-1.

3.7. Martinostat shows synergistic cytotoxicity in combination with imatinib in CML.

In order to investigate whether the apoptosis induced by martinostat in combination with imatinib in CML is synergistic or not, we used sub-toxic concentrations of martinostat and treated K562 and KBM-5 cells in combination with two sub-toxic concentrations of imatinib. Martinostat (0.15 µM) and imatinib (0.15 µM) showed 10 to 15 % apoptotic nuclear fragmentation whereas the combination showed 70 % of apoptotic nuclear fragmentation after 24 h of treatment. Moreover, the combination significantly increased caspase 3/7 activity after 16 h compared to individual treatments.

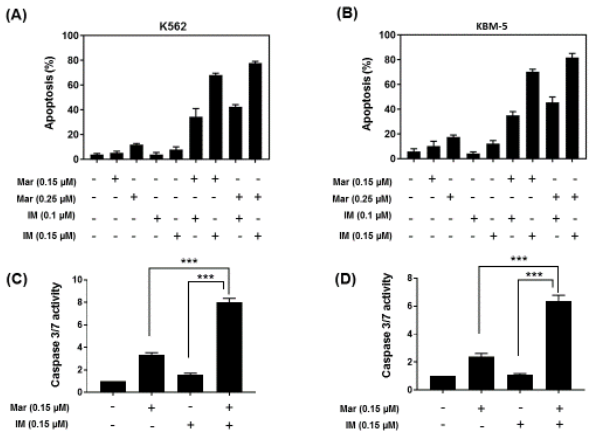

Figure 3. 7: Martinostat synergizes with imatinib in CML.

(A) Apoptosis percent in K562 cells after 24 h. (B) Apoptosis percent in KBM-5 cells after 24 h. (C) Caspase 3/7 activity in K562 cells after 16 h. (D) Caspase 3/7 activity in KBM-5 cells after 16 h. Histogram correspond to the mean ± SD of three independent experiments; ***$p < 0.005$.

3.8. Martinostat re-sensitizes imatinib-resistant cells to imatinib treatment and shows synergistic cytotoxicity

In order to investigate the effect of martinostat in imatinib resistant CML, we used two sub-toxic concentrations of martinostat 0.15 (μM) and 0.25 (μM) in combination with imatinib 0.5 (μM) and 1.0 (μM). The two concentrations of imatinib are pharmacologically effective in CML however, non-effective in resistant CML. Martinostat treatment re-sensitized the resistant cells to imatinib treatment and showed synergistic cytotoxicity in combination after 24 h. Moreover, the combination treatment showed significant increase in caspase 3/7 activation compared to individual treatment after 16 h of treatment.

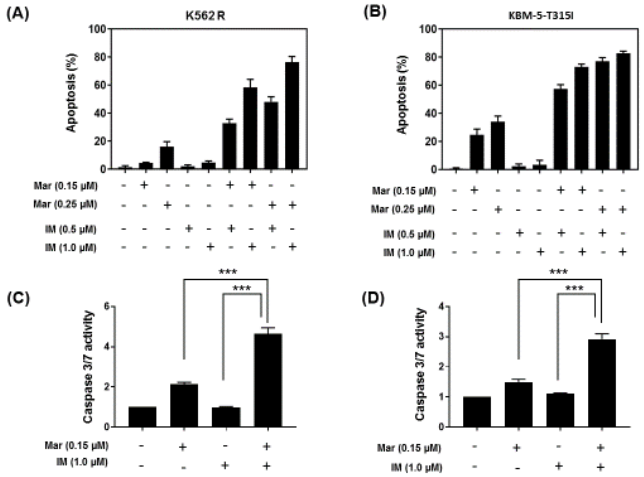

Figure 3. 8: Martinostat re-sensitizes imatinib resistant CML to imatinib.

(A) Apoptosis percent in K562R cells after 24 h. (B) Apoptosis percent in KBM-5-T315I cells after 24 h. (C) Caspase 3/7 activity in K562R cells after 16 h. (D) Caspase 3/7 activity in KBM-5-T315I cells after 16 h. Histogram correspond to the mean ± SD of three independent experiments; ***$p < 0.005$.

3.9. Martinostat in combination with imatinib inhibits colony formation of imatinib-sensitive and –resistant CML

In order to extend our findings in anchorage independent growth of colony formation, we used the sub-toxic concentration of martinostat 0.01 (μM) in combination with imatinb 0.15 (μM) and imatinib 1.0 (μM) for sensitive and –resistant cells respectively. The combination treatment significantly reduced more than 80 % of colonies for both sensitive and -resistant cells.

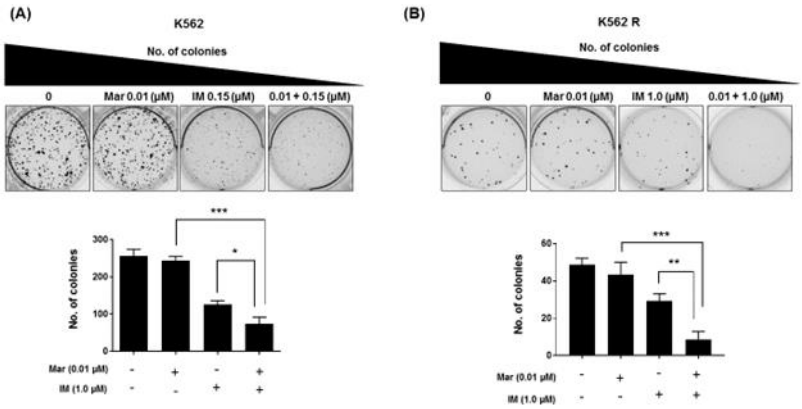

Figure 3. 9. Martinostat and imatinib inhibit CML colony formation.

(A) Colony formation in K562. (B) Colony formation in K562R. Histogram correspond to the mean ± SD of three independent experiments; *p <0.05, **p <0.01, ***p < 0.005.

4. Discussion

The interaction between genome and epigenome is crucial for the development and functioning of eukaryotic cells [50]. The structure and function of epigenome is controlled by specific covalent modifications of chromatin components which include the DNA, RNA and protein (histones). Specific covalent marks are applied by enzymes known as “writers” to the 147 bp of DNA and the eight histone components of a nucleosome. These marks are recognized by a specific class of proteins known as “readers” which are involved in remodeling particular region of genome to regulate gene expression. Another class of enzymes known as erasers hold the function to remove active or repressive marks on a particular region of genome to modulate gene expression. Together the readers, writers and erasers form the core regulators of the epigenome [50].

Next generation sequencing has revealed that 50 % of human cancers show abnormal expression of enzymes which are involved in chromatin organization [50]. It is now well established that cancer cells routinely undergo epigenetic modifications to escape from chemotherapy and host immune surveillance. This has prompted the pharmaceutical industries to identify new molecules which can target epigenetic alterations in a given cancer.

HDACs are involved in regulation of different proteins both during the initiation and progression of cancer [51]. HDACs remove the acetyl group from histones such that the chromatin conformation is non-permissive for transcription of genes. Beside this HDACs also deacetylase a variety of other protein targets including transcription factors and cellular proteins involved in cell proliferation and apoptosis [51].

In CML, histone modifications have been studied since the development of HDAC inhibitors. The first HDAC inhibitor to get FDA approval was vorinostat or SAHA which is approved for the treatment of cutaneous T-cell lymphoma [52]. SAHA was reported to induce the expression of p21 and / or p27 and concomitantly decreased the expression of Bcr-Abl in CML and trigger apoptosis. Our results showed SAHA reduced the viability of CML cells when exposed to a concentration of 2 µM or above. This observation is in line with previously published report, which showed that SAHA reduced the viability of K562 and LAMA-84 starting at a concentration of 2 µM and above after 48 h of treatment [53]. Interestingly the compound martinostat is effective in a concentration range much lower than SAHA and reduced cell proliferation, viability, colony formation and cell cycle arrest in imatinib sensitive and –resistant cells at ten times reduced concentration compared to SAHA.

Previously it was reported that HDAC inhibitor LBH in combination with imatinib reduced engraftment of CML CD34+ cells in mice and was shown to target the quiescent CD34+Bcr-Abl+ cells which are not targeted by the tyrosine kinases [45]. This population of CD34+Bcr-Abl+ cells are responsible for disease relapse after tyrosine kinase therapy. Our results with martinostat and imatinib co-treatment showed that the combination is effective in both imatinib sensitive and –resistant CML. Moreover, inhibition of K562R colony formation by the combination treatment showed that the combination reduced the colony forming ability of ALDH high stem like cells. This suggest that the combination of martinostat and imatinib may be effective in targeting CD34+ Bcr-Abl+ stem like cells and may impair engraftment of these cells in an in vivo setting.

HDAC inhibitors have been used in combination with immune activating antibodies designed to promote the function of antigen presenting cells (APCs) and enhance proliferation and survival of cytotoxic T cells (CTL) to stimulate a host antitumor immune response [54]. However, it would also be interesting to see if HDAC inhibitors themselves promote an immunogenic response which may potentiate the anti-cancer effect when given in combination with conventional chemotherapy or targeted agents. Our experiments show ectopic expression of calreticulin and ERp57 with martinostat treatment suggest that the compound trigger an immunogenic cell death response in CML.

REFERENCES

[1] Y. Sun, Z.L. Peng, Programmed cell death and cancer, Postgrad Med J, 85 (2009) 134-140.

[2] S. Elmore, Apoptosis: a review of programmed cell death, Toxicol Pathol, 35 (2007) 495-516.

[3] N.N. Danial, S.J. Korsmeyer, Cell death: critical control points, Cell, 116 (2004) 205-219.

[4] V.J. Bykov, N. Issaeva, G. Selivanova, K.G. Wiman, Mutant p53-dependent growth suppression distinguishes PRIMA-1 from known anticancer drugs: a statistical analysis of information in the National Cancer Institute database, Carcinogenesis, 23 (2002) 2011-2018.

[5] A. Ashkenazi, W.J. Fairbrother, J.D. Leverson, A.J. Souers, From basic apoptosis discoveries to advanced selective BCL-2 family inhibitors, Nat Rev Drug Discov, 16 (2017) 273-284.

[6] C. Cerella, A. Gaigneaux, A. Mazumder, J.Y. Lee, E. Saland, F. Radogna, T. Farge, F. Vergez, C. Recher, J.E. Sarry, K.W. Kim, H.Y. Shin, M. Dicato, M. Diederich, Bcl-2 protein family expression pattern determines synergistic pro-apoptotic effects of BH3 mimetics with hemisynthetic cardiac glycoside UNBS1450 in acute myeloid leukemia, Leukemia, 31 (2017) 755-759.

[7] G. Manic, F. Obrist, G. Kroemer, I. Vitale, L. Galluzzi, Chloroquine and hydroxychloroquine for cancer therapy, Mol Cell Oncol, 1 (2014) e29911.

[8] M. Conrad, J.P. Angeli, P. Vandenabeele, B.R. Stockwell, Regulated necrosis: disease relevance and therapeutic opportunities, Nat Rev Drug Discov, 15 (2016) 348-366.

[9] P. Scaffidi, T. Misteli, M.E. Bianchi, Release of chromatin protein HMGB1 by necrotic cells triggers inflammation, Nature, 418 (2002) 191-195.

[10] S. Park, H. Shin, Y. Cho, Shikonin induces programmed necrosis-like cell death through the formation of receptor interacting protein 1 and 3 complex, Food Chem Toxicol, 55 (2013) 36-41.

[11] R. Kim, M. Emi, K. Tanabe, Cancer immunoediting from immune surveillance to immune escape, Immunology, 121 (2007) 1-14.

[12] G. Kroemer, L. Galluzzi, O. Kepp, L. Zitvogel, Immunogenic cell death in cancer therapy, Annu Rev Immunol, 31 (2013) 51-72.

[13] L. Galluzzi, A. Buque, O. Kepp, L. Zitvogel, G. Kroemer, Immunogenic cell death in cancer and infectious disease, Nat Rev Immunol, 17 (2017) 97-111.

[14] L. Zitvogel, O. Kepp, G. Kroemer, Immune parameters affecting the efficacy of chemotherapeutic regimens, Nat Rev Clin Oncol, 8 (2011) 151-160.

[15] L. Apetoh, F. Ghiringhelli, A. Tesniere, M. Obeid, C. Ortiz, A. Criollo, G. Mignot, M.C. Maiuri, E. Ullrich, P. Saulnier, H. Yang, S. Amigorena, B. Ryffel, F.J. Barrat, P. Saftig, F. Levi, R. Lidereau, C. Nogues, J.P. Mira, A.

Chompret, V. Joulin, F. Clavel-Chapelon, J. Bourhis, F. Andre, S. Delaloge, T. Tursz, G. Kroemer, L. Zitvogel, Toll-like receptor 4-dependent contribution of the immune system to anticancer chemotherapy and radiotherapy, Nat Med, 13 (2007) 1050-1059.

[16] T. Panaretakis, N. Joza, N. Modjtahedi, A. Tesniere, I. Vitale, M. Durchschlag, G.M. Fimia, O. Kepp, M. Piacentini, K.U. Froehlich, P. van Endert, L. Zitvogel, F. Madeo, G. Kroemer, The co-translocation of ERp57 and calreticulin determines the immunogenicity of cell death, Cell Death Differ, 15 (2008) 1499-1509.

[17] R. Zappasodi, S.M. Pupa, G.C. Ghedini, I. Bongarzone, M. Magni, A.D. Cabras, M.P. Colombo, C. Carlo-Stella, A.M. Gianni, M. Di Nicola, Improved clinical outcome in indolent B-cell lymphoma patients vaccinated with autologous tumor cells experiencing immunogenic death, Cancer Res, 70 (2010) 9062-9072.

[18] M. Wemeau, O. Kepp, A. Tesniere, T. Panaretakis, C. Flament, S. De Botton, L. Zitvogel, G. Kroemer, N. Chaput, Calreticulin exposure on malignant blasts predicts a cellular anticancer immune response in patients with acute myeloid leukemia, Cell Death Dis, 1 (2010) e104.

[19] M.R. Elliott, F.B. Chekeni, P.C. Trampont, E.R. Lazarowski, A. Kadl, S.F. Walk, D. Park, R.I. Woodson, M. Ostankovich, P. Sharma, J.J. Lysiak, T.K. Harden, N. Leitinger, K.S. Ravichandran, Nucleotides released by

apoptotic cells act as a find-me signal to promote phagocytic clearance, Nature, 461 (2009) 282-286.

[20] M. Kronlage, J. Song, L. Sorokin, K. Isfort, T. Schwerdtle, J. Leipziger, B. Robaye, P.B. Conley, H.C. Kim, S. Sargin, P. Schon, A. Schwab, P.J. Hanley, Autocrine purinergic receptor signaling is essential for macrophage chemotaxis, Sci Signal, 3 (2010) ra55.

[21] R.D. Granstein, W. Ding, J. Huang, A. Holzer, R.L. Gallo, A. Di Nardo, J.A. Wagner, Augmentation of cutaneous immune responses by ATP gamma S: purinergic agonists define a novel class of immunologic adjuvants, J Immunol, 174 (2005) 7725-7731.

[22] J. Cortes, H. Kantarjian, Chronic myeloid leukemia: sequencing of TKI therapies, Hematology Am Soc Hematol Educ Program, 2016 (2016) 164-169.

[23] R. Ciarcia, S. Damiano, M.V. Puzio, S. Montagnaro, F. Pagnini, C. Pacilio, G. Caparrotti, C. Bellan, T. Garofano, M.S. Polito, A. Giordano, S. Florio, Comparison of Dasatinib, Nilotinib, and Imatinib in the Treatment of Chronic Myeloid Leukemia, J Cell Physiol, 231 (2016) 680-687.

[24] A. Tarafdar, L.E. Hopcroft, P. Gallipoli, F. Pellicano, J. Cassels, A. Hair, K. Korfi, H.G. Jorgensen, D. Vetrie, T.L. Holyoake, A.M. Michie, CML cells actively evade host immune surveillance through cytokine-mediated downregulation of MHC-II expression, Blood, 129 (2017) 199-208.

[25] G. Visani, A. Isidori, Resistant chronic myeloid leukemia beyond tyrosine-kinase inhibitor therapy: which role for omacetaxine?, Expert Opin Pharmacother, 15 (2014) 1-3.

[26] G.D. Miller, B.J. Bruno, C.S. Lim, Resistant mutations in CML and Ph(+)ALL - role of ponatinib, Biologics, 8 (2014) 243-254.

[27] A.S. Corbin, A. Agarwal, M. Loriaux, J. Cortes, M.W. Deininger, B.J. Druker, Human chronic myeloid leukemia stem cells are insensitive to imatinib despite inhibition of BCR-ABL activity, J Clin Invest, 121 (2011) 396-409.

[28] Z. Zou, B. Huang, X. Wu, H. Zhang, J. Qi, J. Bradner, S. Nair, L.F. Chen, Brd4 maintains constitutively active NF-kappaB in cancer cells by binding to acetylated RelA, Oncogene, 33 (2014) 2395-2404.

[29] O. Talhi, M. Schnekenburger, J. Panning, D.G. Pinto, J.A. Fernandes, F.A. Almeida Paz, C. Jacob, M. Diederich, A.M. Silva, Bis(4-hydroxy-2H-chromen-2-one): synthesis and effects on leukemic cell lines proliferation and NF-kappaB regulation, Bioorg Med Chem, 22 (2014) 3008-3015.

[30] K. Kono, K. Mimura, R. Kiessling, Immunogenic tumor cell death induced by chemoradiotherapy: molecular mechanisms and a clinical translation, Cell Death Dis, 4 (2013) e688.

[31] G. Schiavoni, A. Sistigu, M. Valentini, F. Mattei, P. Sestili, F. Spadaro, M. Sanchez, S. Lorenzi, M.T. D'Urso, F. Belardelli, L. Gabriele, E. Proietti, L.

Bracci, Cyclophosphamide synergizes with type I interferons through systemic dendritic cell reactivation and induction of immunogenic tumor apoptosis, Cancer Res, 71 (2011) 768-778.

[32] C. Borg, M. Terme, J. Taieb, C. Menard, C. Flament, C. Robert, K. Maruyama, H. Wakasugi, E. Angevin, K. Thielemans, A. Le Cesne, V. Chung-Scott, V. Lazar, I. Tchou, F. Crepineau, F. Lemoine, J. Bernard, J.A. Fletcher, A. Turhan, J.Y. Blay, A. Spatz, J.F. Emile, M.C. Heinrich, S. Mecheri, T. Tursz, L. Zitvogel, Novel mode of action of c-kit tyrosine kinase inhibitors leading to NK cell-dependent antitumor effects, J Clin Invest, 114 (2004) 379-388.

[33] M. Bar-Natan, E.A. Nelson, M. Xiang, D.A. Frank, STAT signaling in the pathogenesis and treatment of myeloid malignancies, JAKSTAT, 1 (2012) 55-64.

[34] S. Bibi, M.D. Arslanhan, F. Langenfeld, S. Jeanningros, S. Cerny-Reiterer, E. Hadzijusufovic, L. Tchertanov, R. Moriggl, P. Valent, M. Arock, Co-operating STAT5 and AKT signaling pathways in chronic myeloid leukemia and mastocytosis: possible new targets of therapy, Haematologica, 99 (2014) 417-429.

[35] S. Prost, F. Relouzat, M. Spentchian, Y. Ouzegdouh, J. Saliba, G. Massonnet, J.P. Beressi, E. Verhoeyen, V. Raggueneau, B. Maneglier, S. Castaigne, C. Chomienne, S. Chretien, P. Rousselot, P. Leboulch, Erosion of

the chronic myeloid leukaemia stem cell pool by PPARgamma agonists, Nature, 525 (2015) 380-383.

[36] T. Braun, G. Carvalho, C. Fabre, J. Grosjean, P. Fenaux, G. Kroemer, Targeting NF-kappaB in hematologic malignancies, Cell Death Differ, 13 (2006) 748-758.

[37] F.E. Nicolini, H.J. Khoury, L. Akard, D. Rea, H. Kantarjian, M. Baccarani, J. Leonoudakis, A. Craig, A.C. Benichou, J. Cortes, Omacetaxine mepesuccinate for patients with accelerated phase chronic myeloid leukemia with resistance or intolerance to two or more tyrosine kinase inhibitors, Haematologica, 98 (2013) e78-79.

[38] E.K. Allan, T.L. Holyoake, A.R. Craig, H.G. Jorgensen, Omacetaxine may have a role in chronic myeloid leukaemia eradication through downregulation of Mcl-1 and induction of apoptosis in stem/progenitor cells, Leukemia, 25 (2011) 985-994.

[39] J.T. Leonard, J.S. Rowley, C.A. Eide, E. Traer, B. Hayes-Lattin, M. Loriaux, S.E. Spurgeon, B.J. Druker, J.W. Tyner, B.H. Chang, Targeting BCL-2 and ABL/LYN in Philadelphia chromosome-positive acute lymphoblastic leukemia, Sci Transl Med, 8 (2016) 354ra114.

[40] X. Xu, S. Chai, P. Wang, C. Zhang, Y. Yang, Y. Yang, K. Wang, Aldehyde dehydrogenases and cancer stem cells, Cancer Lett, 369 (2015) 50-57.

[41] E.M. Kuntz, P. Baquero, A.M. Michie, K. Dunn, S. Tardito, T.L. Holyoake, G.V. Helgason, E. Gottlieb, Targeting mitochondrial oxidative phosphorylation eradicates therapy-resistant chronic myeloid leukemia stem cells, Nat Med, 23 (2017) 1234-1240.

[42] D. Theile, N. Hohmann, D. Kiemel, G. Gattuso, D. Barreca, G. Mikus, W.E. Haefeli, V. Schwenger, J. Weiss, Clementine juice has the potential for drug interactions - In vitro comparison with grapefruit and mandarin juice, Eur J Pharm Sci, 97 (2017) 247-256.

[43] M. Copland, F. Pellicano, L. Richmond, E.K. Allan, A. Hamilton, F.Y. Lee, R. Weinmann, T.L. Holyoake, BMS-214662 potently induces apoptosis of chronic myeloid leukemia stem and progenitor cells and synergizes with tyrosine kinase inhibitors, Blood, 111 (2008) 2843-2853.

[44] N.B. Heaney, F. Pellicano, B. Zhang, L. Crawford, S. Chu, S.M. Kazmi, E.K. Allan, H.G. Jorgensen, A.E. Irvine, R. Bhatia, T.L. Holyoake, Bortezomib induces apoptosis in primitive chronic myeloid leukemia cells including LTC-IC and NOD/SCID repopulating cells, Blood, 115 (2010) 2241-2250.

[45] B. Zhang, A.C. Strauss, S. Chu, M. Li, Y. Ho, K.D. Shiang, D.S. Snyder, C.S. Huettner, L. Shultz, T. Holyoake, R. Bhatia, Effective targeting of quiescent chronic myelogenous leukemia stem cells by histone deacetylase

inhibitors in combination with imatinib mesylate, Cancer Cell, 17 (2010) 427-442.

[46] C. Sawan, Z. Herceg, Histone modifications and cancer, Adv Genet, 70 (2010) 57-85.

[47] P. George, P. Bali, S. Annavarapu, A. Scuto, W. Fiskus, F. Guo, C. Sigua, G. Sondarva, L. Moscinski, P. Atadja, K. Bhalla, Combination of the histone deacetylase inhibitor LBH589 and the hsp90 inhibitor 17-AAG is highly active against human CML-BC cells and AML cells with activating mutation of FLT-3, Blood, 105 (2005) 1768-1776.

[48] E.J. Jabbour, J.E. Cortes, H.M. Kantarjian, Resistance to tyrosine kinase inhibition therapy for chronic myelogenous leukemia: a clinical perspective and emerging treatment options, Clin Lymphoma Myeloma Leuk, 13 (2013) 515-529.

[49] P.V. Licciardi, T.C. Karagiannis, Regulation of immune responses by histone deacetylase inhibitors, ISRN Hematol, 2012 (2012) 690901.

[50] P.A. Jones, J.P. Issa, S. Baylin, Targeting the cancer epigenome for therapy, Nat Rev Genet, 17 (2016) 630-641.

[51] M.A. Glozak, E. Seto, Histone deacetylases and cancer, Oncogene, 26 (2007) 5420-5432.

[52] K. Machova Polakova, J. Koblihova, T. Stopka, Role of epigenetics in chronic myeloid leukemia, Curr Hematol Malig Rep, 8 (2013) 28-36.

[53] R. Nimmanapalli, L. Fuino, C. Stobaugh, V. Richon, K. Bhalla, Cotreatment with the histone deacetylase inhibitor suberoylanilide hydroxamic acid (SAHA) enhances imatinib-induced apoptosis of Bcr-Abl-positive human acute leukemia cells, Blood, 101 (2003) 3236-3239.

[54] A.C. West, M.J. Smyth, R.W. Johnstone, The anticancer effects of HDAC inhibitors require the immune system, Oncoimmunology, 3 (2014) e27414.

ABSTRACT IN KOREAN

면역 원성 세포 사멸 (Immunogenic cell death, ICD)은 면역 체계의 적응력있는 팔에 관여하는 일련의 사건으로 나타났습니다. 초기 자극에 따라 암 세포 사멸은 세포 표면의 변화와 손상 관련 분자 패턴의 방출과 관련된 일련의 사건을 특징으로하는 ICD 로 정의 할 수 있습니다. 이 현상은 암에 대항하여 작용하는 면역계의 대 식세포 및 수지상 세포를 관여시킵니다.

본 연구에서는 만성 골수성 백혈병 (CML) 세포에서 bis (4- hydroxycoumarin) 유도체 인 OT-55 와 histone

deacetylase inhibitor martinostat 가 소포체 ER 응력에 따라 ICD 를 유발한다는 것을 발견했다. 우리는 T315I 돌연변이가있는 세포에서 ICD 유도의 첫 번째 시연을 제공합니다. OT-55 는 종양 괴사 인자 α에 의해 유도된 핵 인자 -κB 의 활성화를 억제하고, 생체 내 제브라피쉬 모델에서 CML 일차 폭발에 의해 종양 형성을 억제하기 위해 이마티닙과 함께 사용될 때 상승 효과를 나타냈다. 또한 OT-55 는 T315I 돌연변이 세포에서 omacetaxine 과 상승 작용하여 골수 세포 백혈병 1 의 발현을 억제함으로써 세포 사멸을 유발한다. OT-55 는 상승 된 알데하이드 탈수소 효소

활성 및 미토콘드리아 산화 대사를 약화시킴으로써 줄기 유사 특성을 갖는 CML 세포를 표적으로 삼았다. vorinostat 와 비교하여, 마티노 스탯은 아세틸 화 수준을 증가시키고, 세포 증식, 생존력 및 CML 세포의 콜로니 형성을 훨씬 낮은 농도로 증가시켰다. 이마티닙 감수성 및 내성 CML 세포 모두에서 이마 닙과 함께 시너지 효과가 나타났다.